

The role of nitrogen species in atmospheric chemistry

Didier Hauglustaine

**Laboratoire des Sciences du Climat et de l'Environnement (LSCE), Gif-sur-Yvette
Laboratoire Image Ville Environnement (LIVE), Strasbourg**

Anthropogenic perturbation of both the carbon and nitrogen cycle



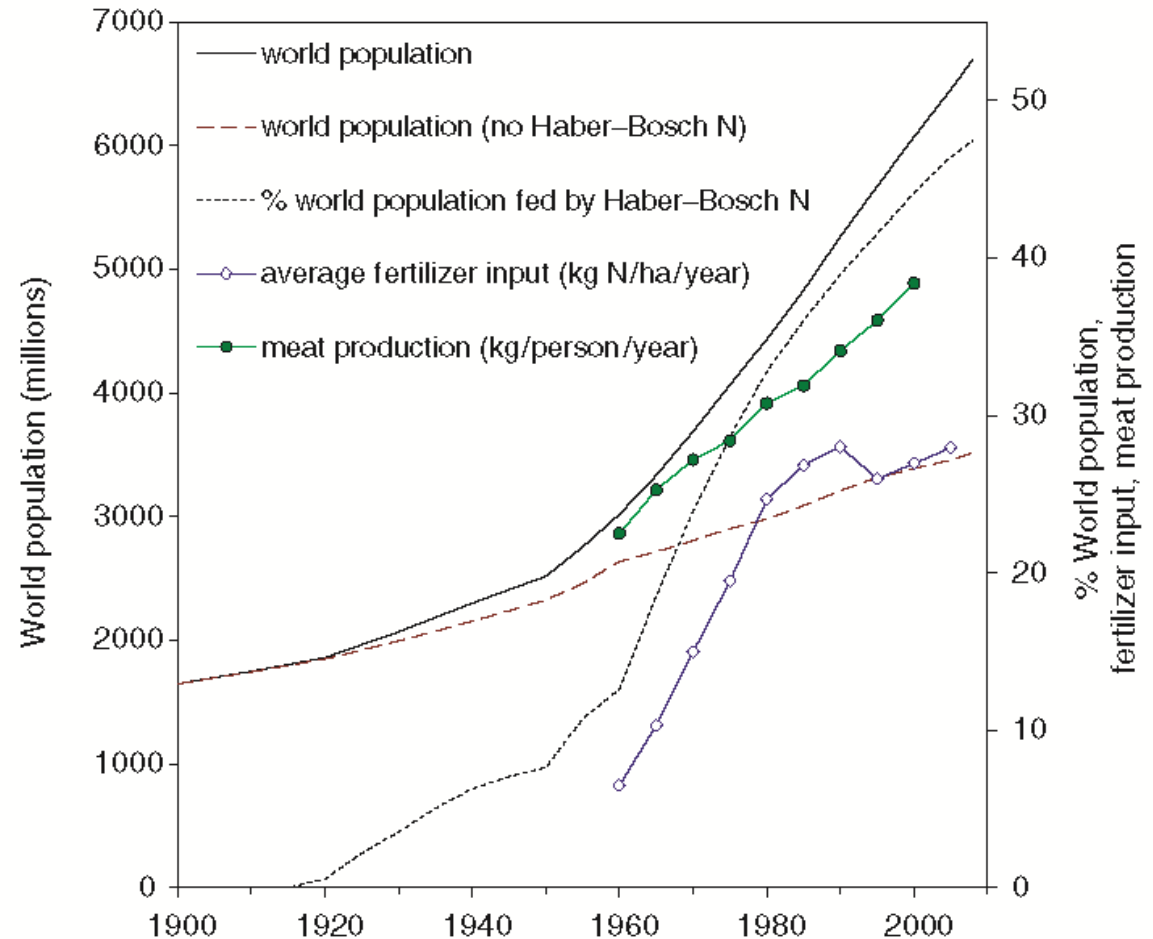
L'invention de la machine à vapeur par J. Watt et l'utilisation du charbon comme source d'énergie marque au XVIII^e siècle le début de la révolution industrielle et l'utilisation des combustibles fossiles.

La mise au point du procédé Haber-Bosch en 1913 permet de synthétiser NH_3 et engrais azotés à partir de N_2 de l'air .



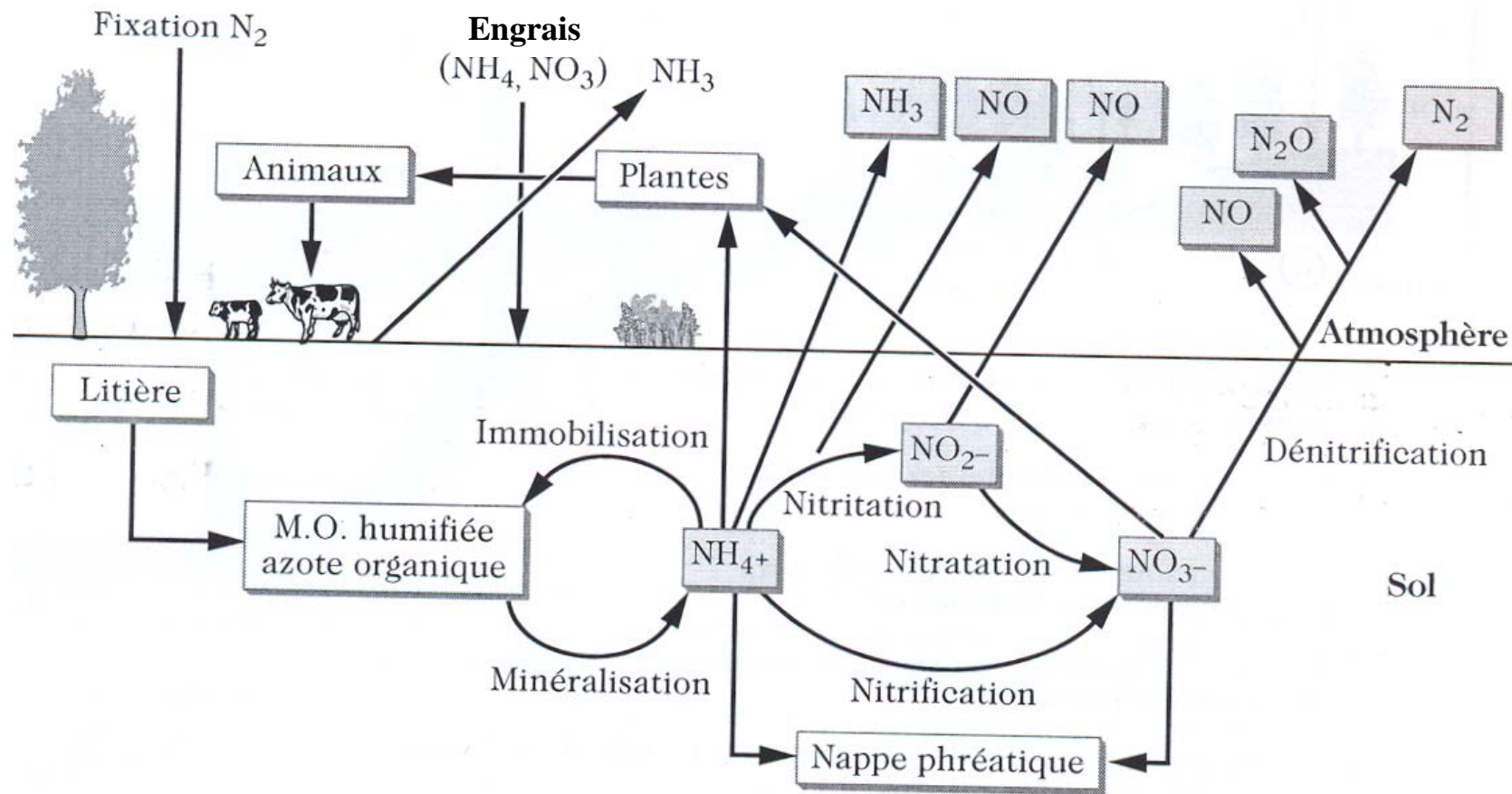
The Haber-Bosch process to feed a growing population

Following the invention of the Haber-Bosch process (1913), it has been possible to produce ammonia in large quantities and relatively cheaply from N_2 . The use of synthetic fertilizers supports about 50% of the world population. In particular, the widespread use of ammonia and its derivative as agricultural nitrogen fertilizers has substantially increased emissions of ammonia in the atmosphere.



European Nitrogen Assessment, 2011

Nitrogen cycle and the role of soils



Le cycle de l'azote dans le sol et productions gazeuses associées.

The nitrogen cascade in the environment

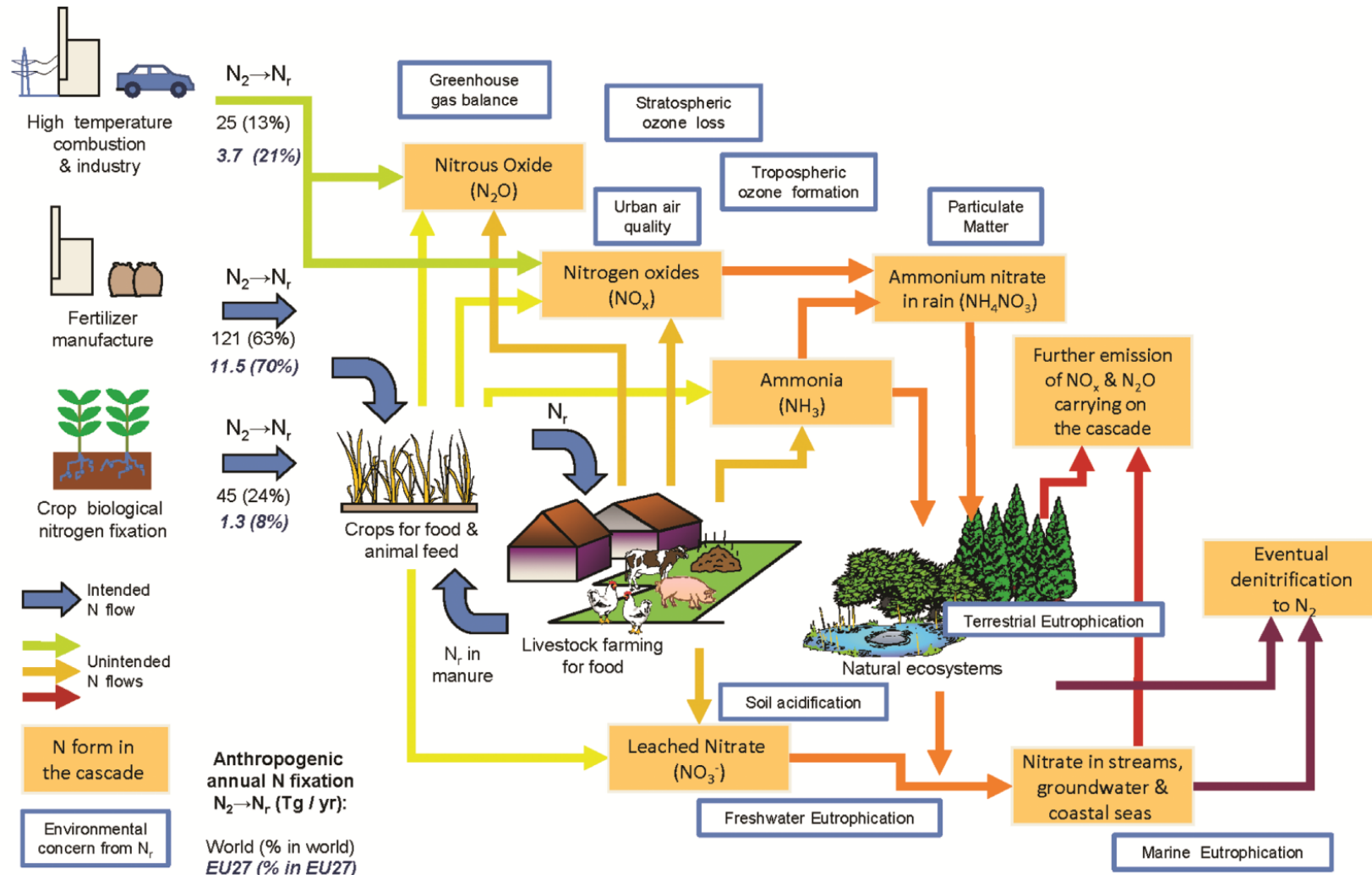
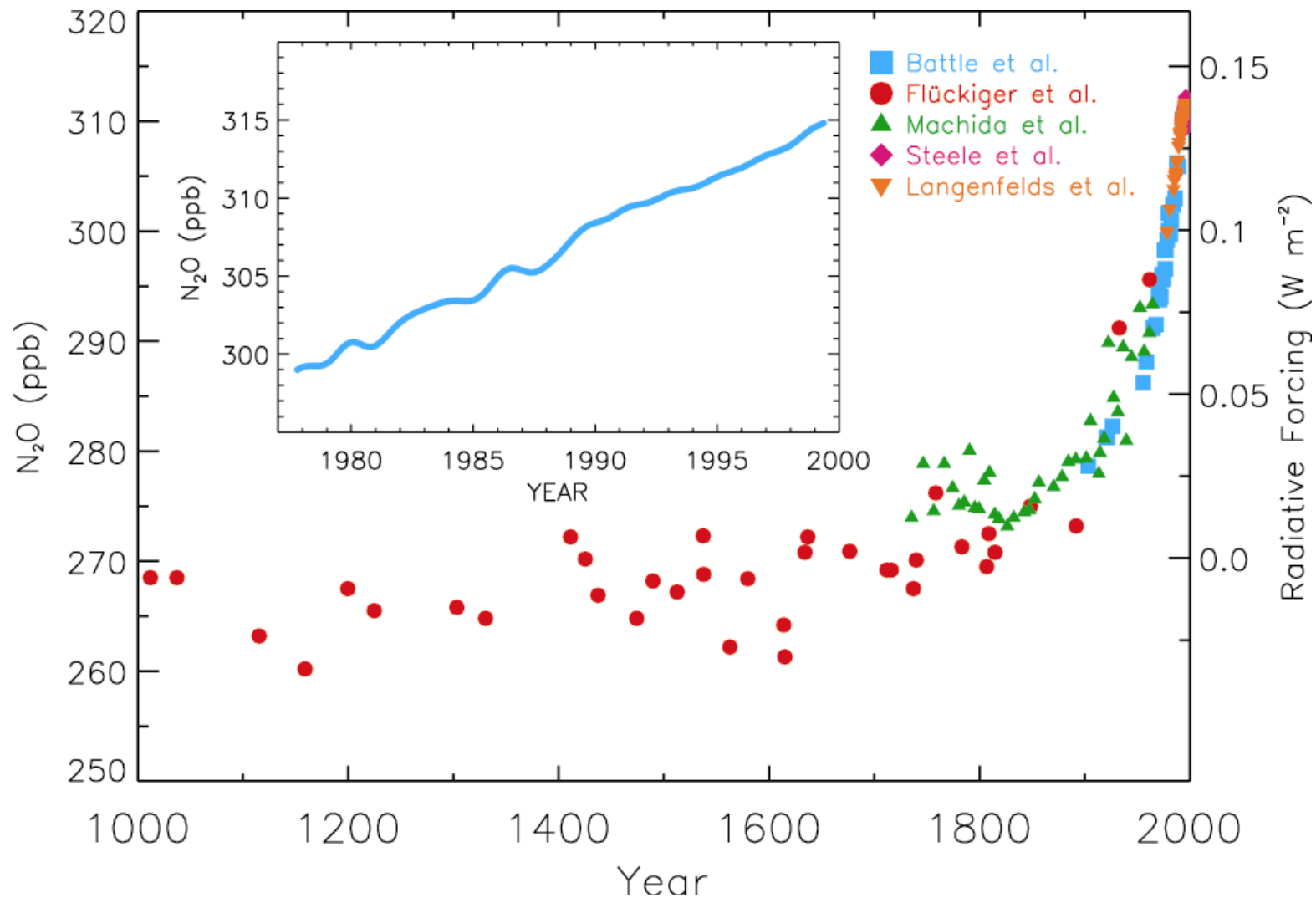


Figure 5.3 Simplified view of the nitrogen cascade, highlighting the major anthropogenic sources of reactive nitrogen (N_r) from atmospheric di-nitrogen (N_2), the main pollutant forms of N_r (orange boxes) and nine main environmental concerns (boxes outlined with blue). Estimates of N fixation for the world (Tg / yr for 2005, in black; Galloway *et al.*, 2008) are compared with estimates for Europe (Tg / yr for 2000, in blue italic; Leip *et al.*, 2011, Chapter 16 this volume). Energy is needed to fix N_2 to N_r , which is gradually dissipated through the cascade with eventual denitrification back to N_2 . Blue arrows represent intended anthropogenic N_r flows; all the other arrows are unintended flows.

Sources of nitrogen species to the atmosphere (TgN/year)

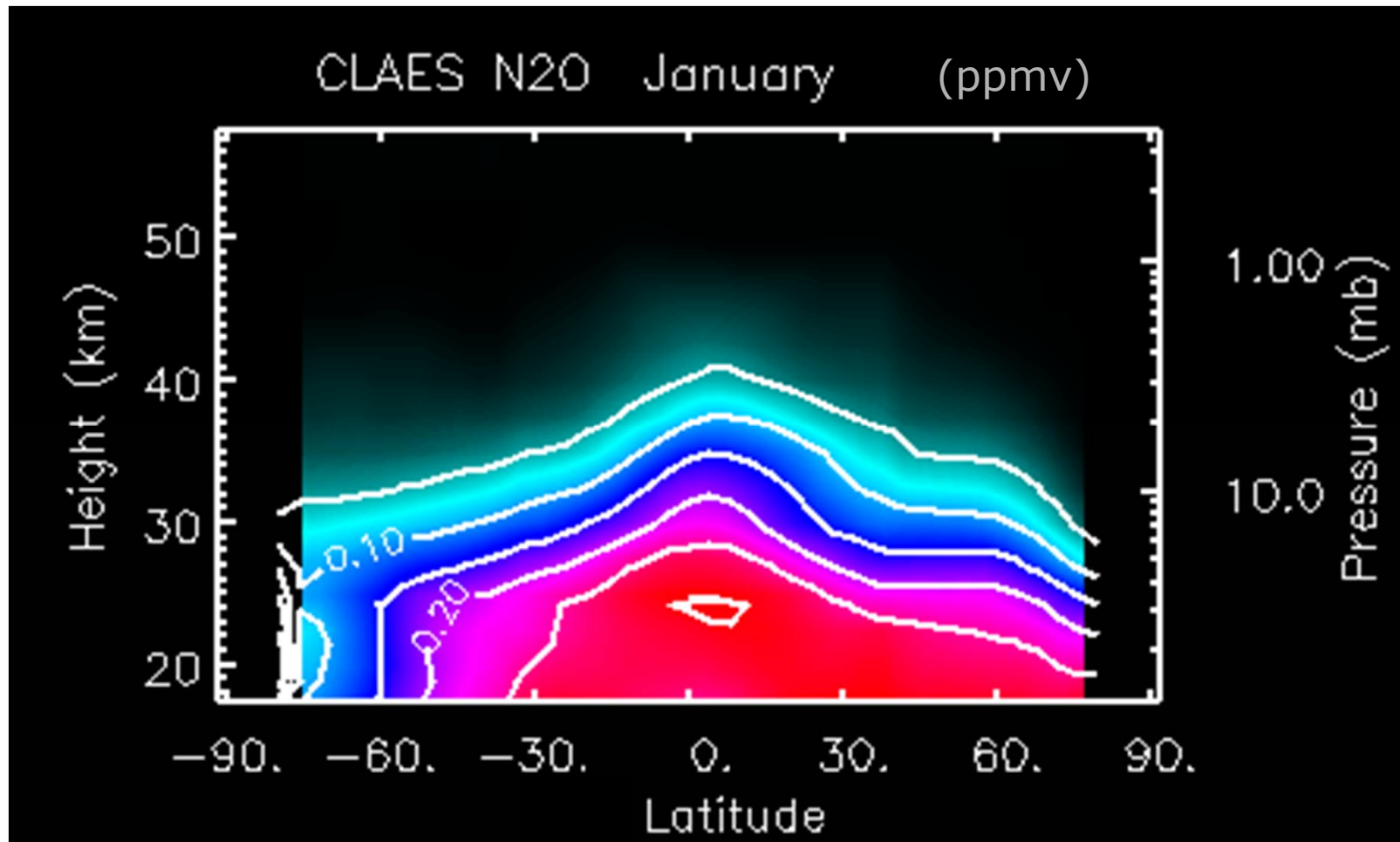
| Sources (TgN/yr) | N ₂ O | NO | NH ₃ |
|--------------------------------------|------------------|-----------|-----------------|
| Natural | | | |
| Oceans | 2 | | 8.2 |
| Soils | 4.5 | 6 | 2.4 |
| Wild animals | | 4 | 0.1 |
| Lightning | | 4 | |
| Total natural sources | 6.5 | 14 | 10.7 |
| Anthropogenic | | | |
| Fossil fuel combustion | 1.2 | 22 | 0.1 |
| Biomass burning | 0.5 | 7 | 5.7 |
| Fertilized soils | 6.3 | 4 | 9.0 |
| Crops | | | 3.6 |
| Domestic animals | | | 21.6 |
| Total anthropogenic sources | 8 | 33 | 40 |
| Total anthropogenic + natural | 14.5 | 47 | 50.7 |

Stratospheric nitrogen - Nitrous oxide, N₂O



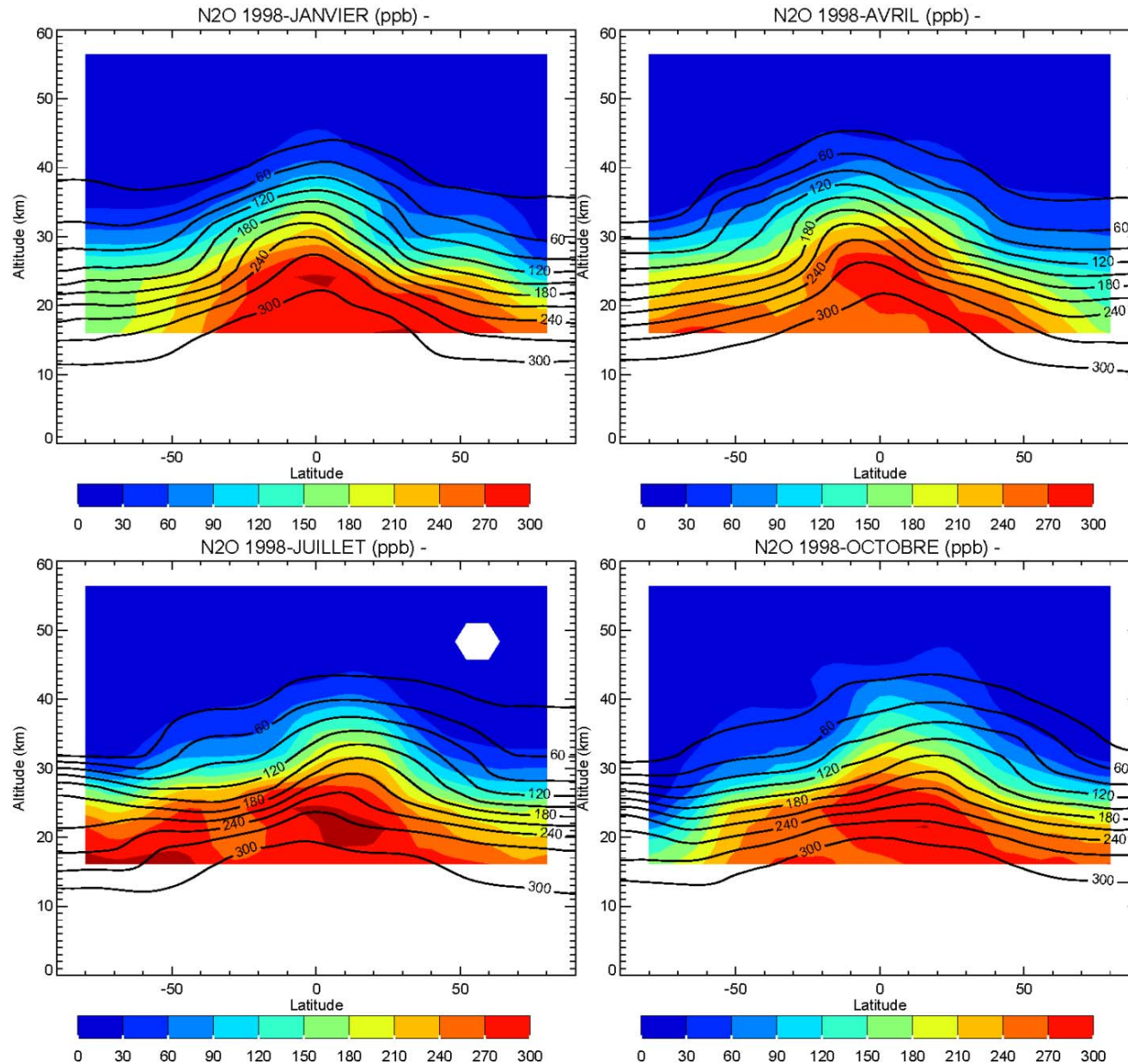
Evolution of N₂O mixing ratio over the last millenium (ppb).

Stratospheric nitrogen - Nitrous oxide, N₂O



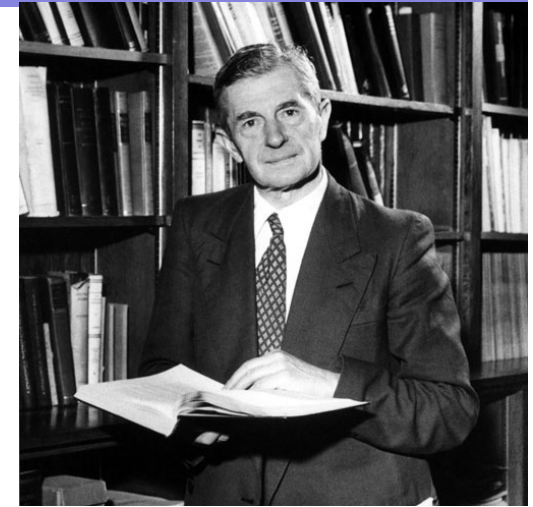
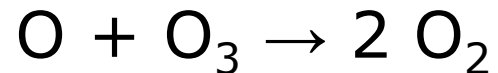
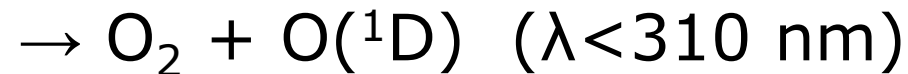
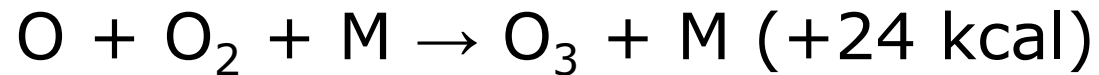
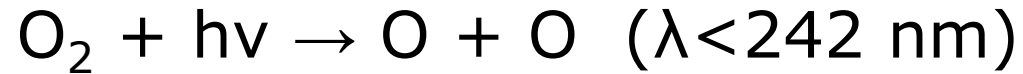
Coupe zonale de N₂O mesurée par l'instrument CLAES.

Nitrous oxide distribution



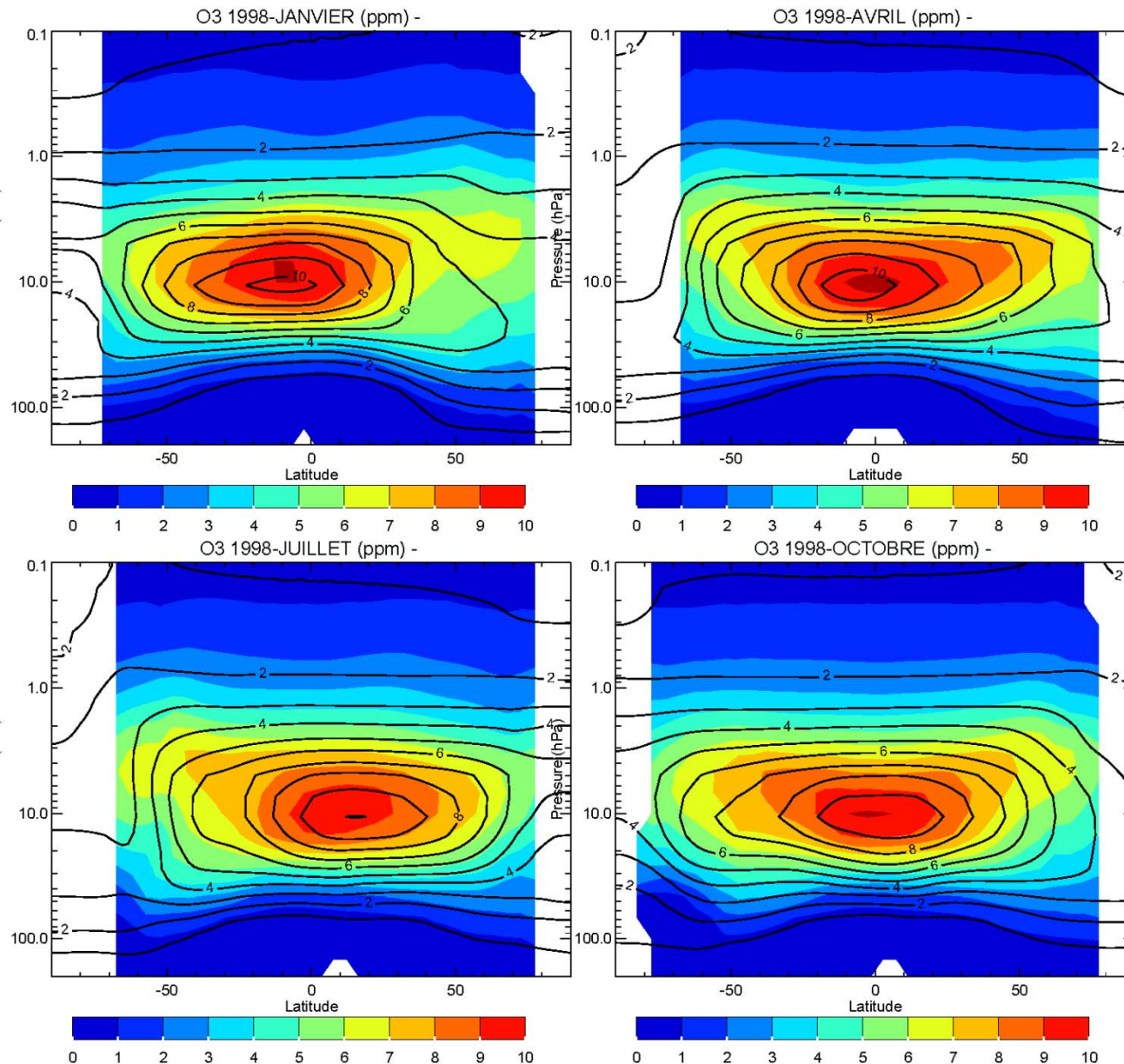
LMDz-INCA isolines
CLAES/UARS colors

Stratospheric ozone : the Chapman cycle



Sydney Chapman
Géophysicien britannique
(1888-1970)

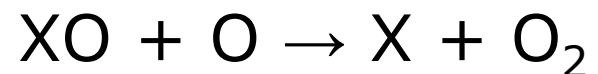
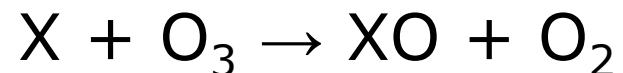
Stratospheric ozone distribution



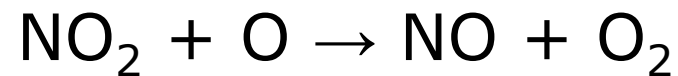
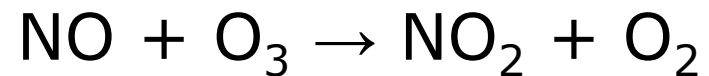
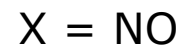
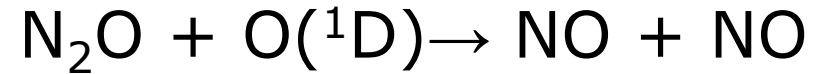
LMDz-INCA isolines
CLAES/UARS colors

Catalytic destruction of stratospheric ozone

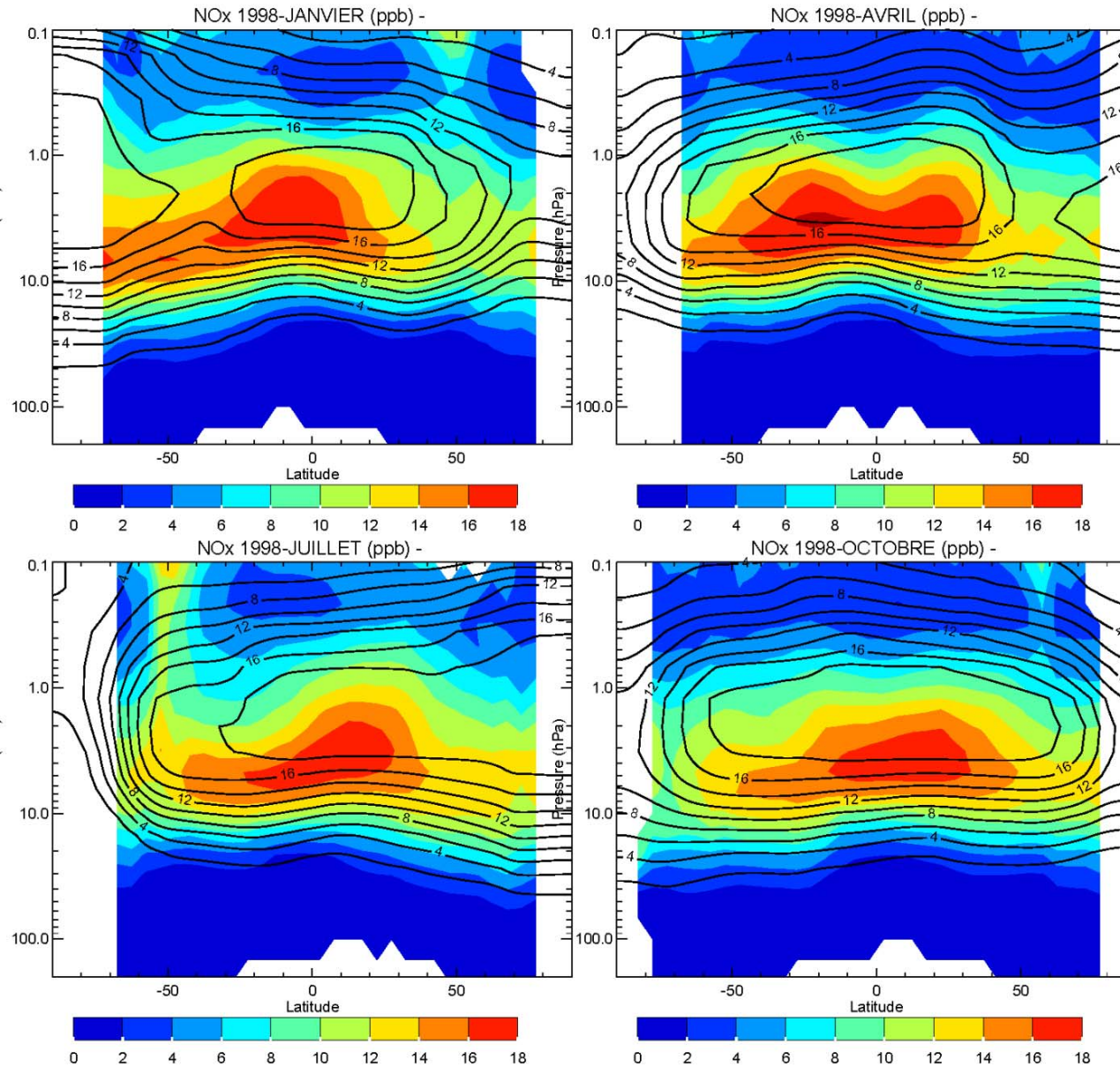
Le cycle de Chapman ne permet pas de reproduire complètement les observations d'ozone.



Catalytic destruction of stratospheric ozone by NO_x



Stratospheric NO_x distribution



Nitrous Oxide : the Dominant Ozone-Depleting Substance Emitted in the 21st Century

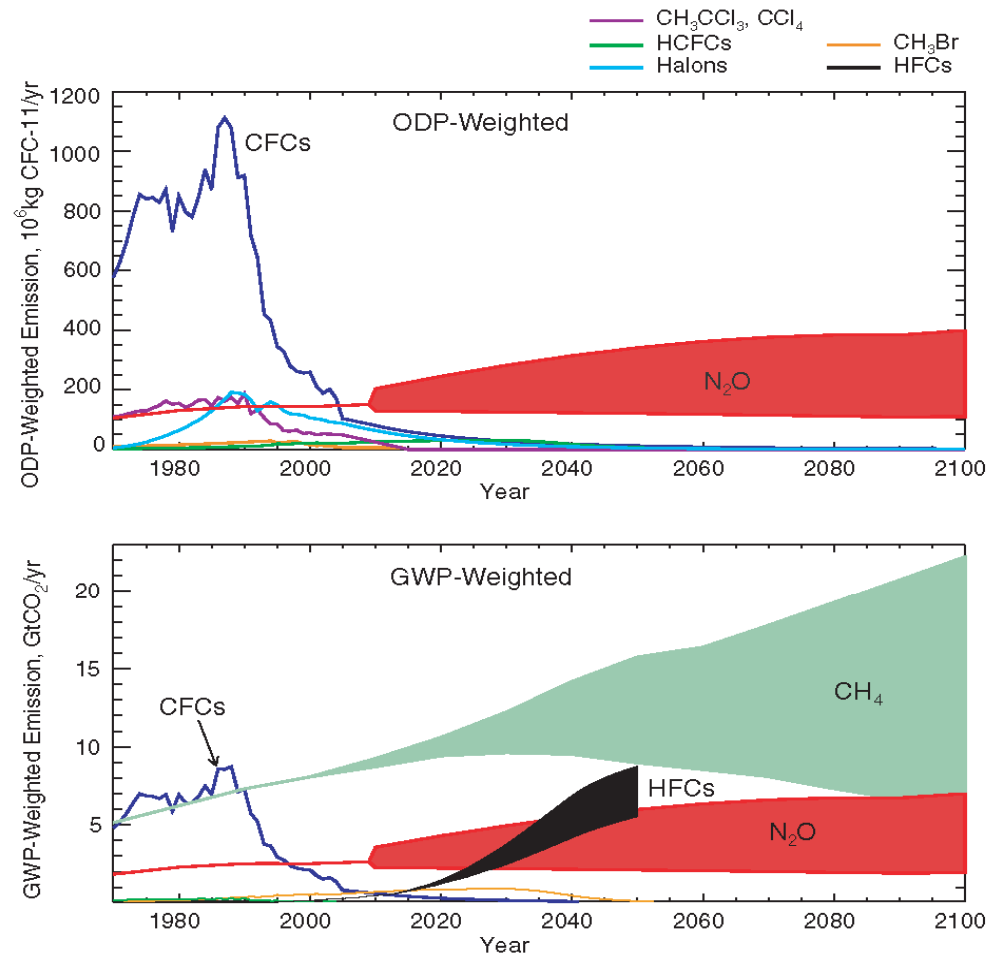


Fig. 2. Historical and projected ODP- and GWP-weighted emissions of the most important ODSs and non- CO_2 greenhouse gases. Non- N_2O ODS emissions are taken from WMO (3). Hydrofluorocarbon (HFC) projections are taken from Velders *et al.* (24), do not include HFC-23, and are estimated assuming unmitigated growth. The HFC band thus represents a likely upper limit for the contribution of HFCs to GWP-weighted emissions. CH_4 emissions represent the range of the Special Report on Emissions scenarios (SRES) A1B, A1T, A1FI, A2, and B1 scenarios (23). The range of anthropogenic N_2O emissions is inferred from the mixing ratios of these same SRES scenarios [see (13) for details of calculation].

Ravishankara et al., Science, 2009.

In the troposphere: anthropogenic NO_x emissions

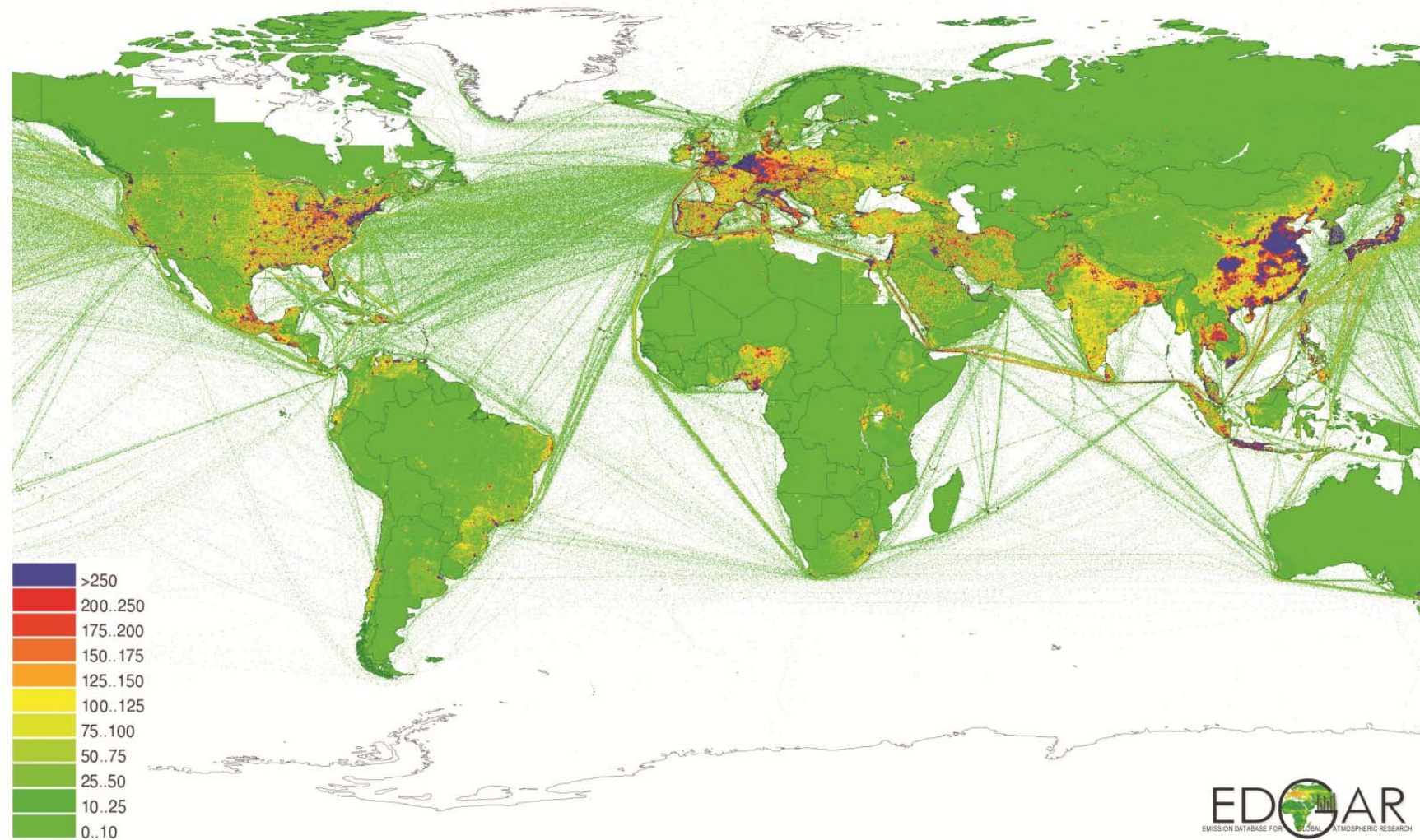
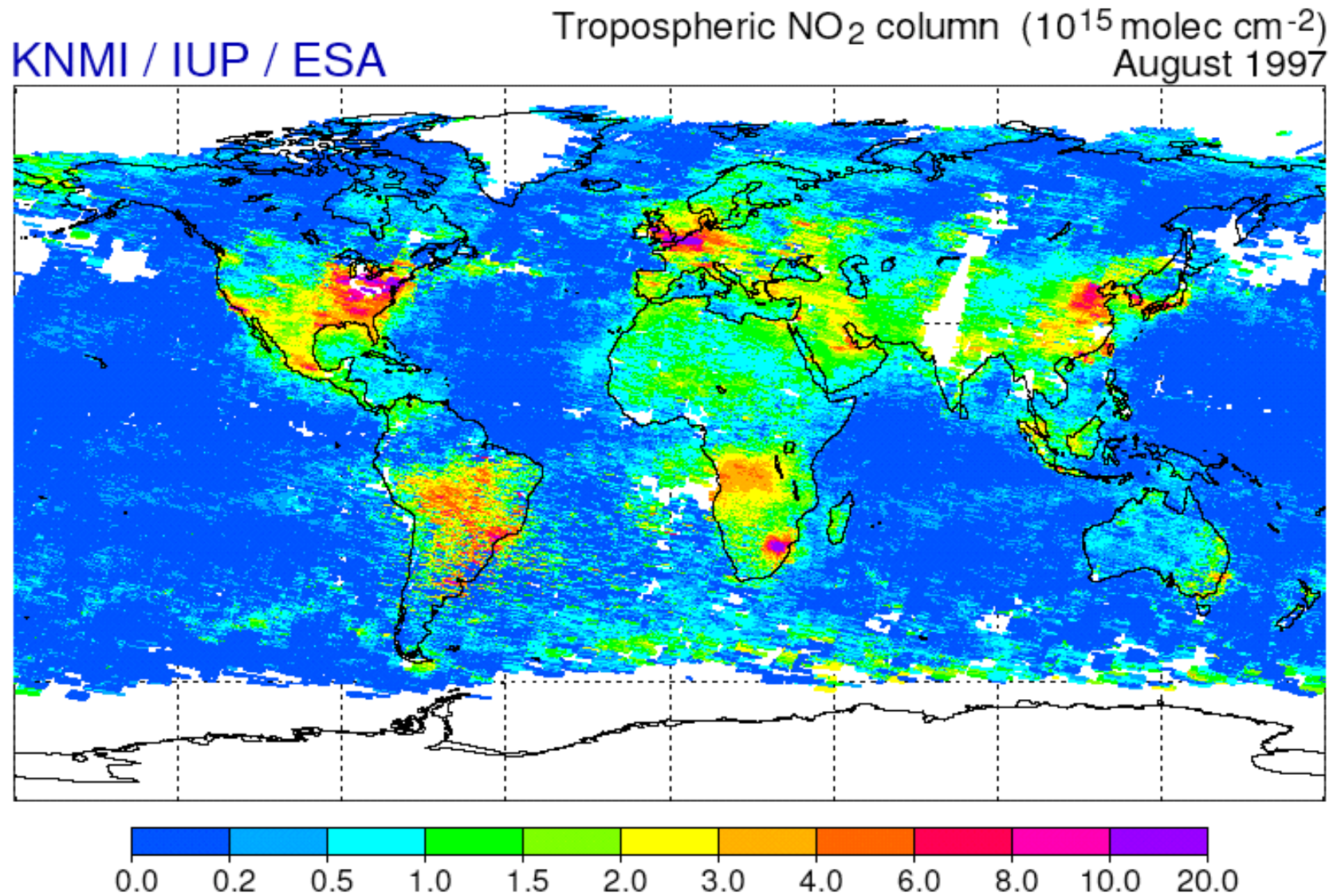


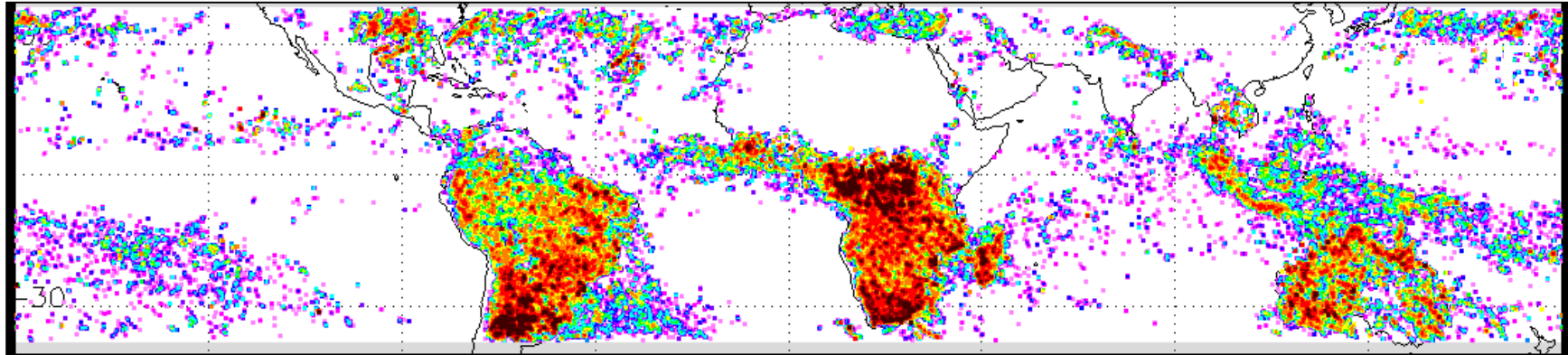
Figure 2.8 Global emissions of nitrogen oxides (NO_x) (EDGAR, 2010).

NO₂ column observed from space

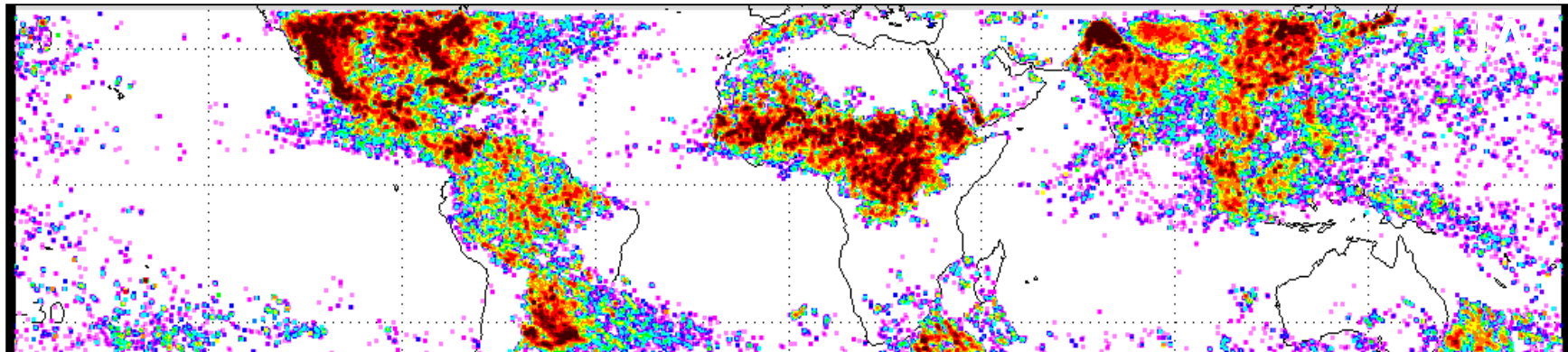


Lightning flashes observed from space

Janvier

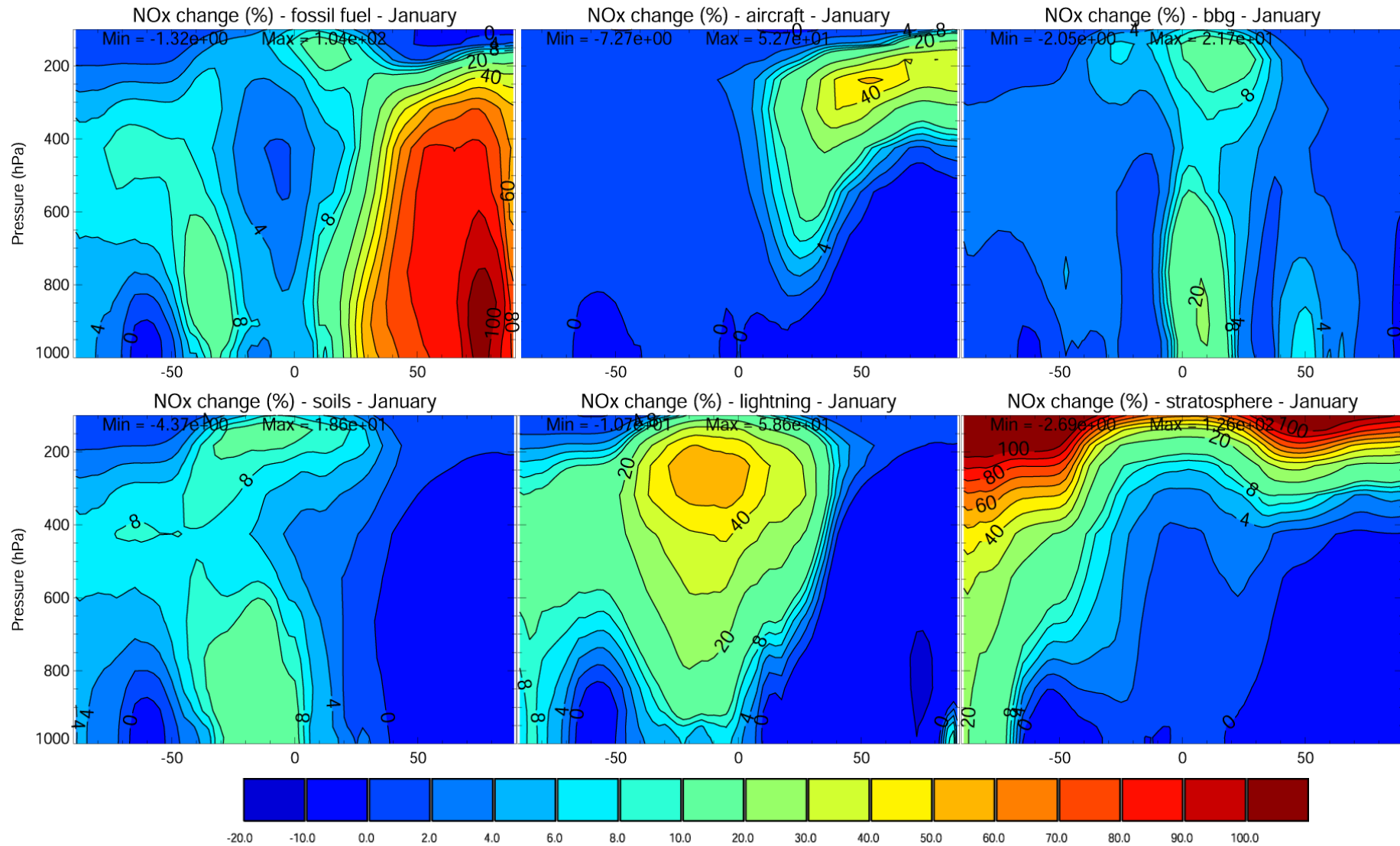


Juillet



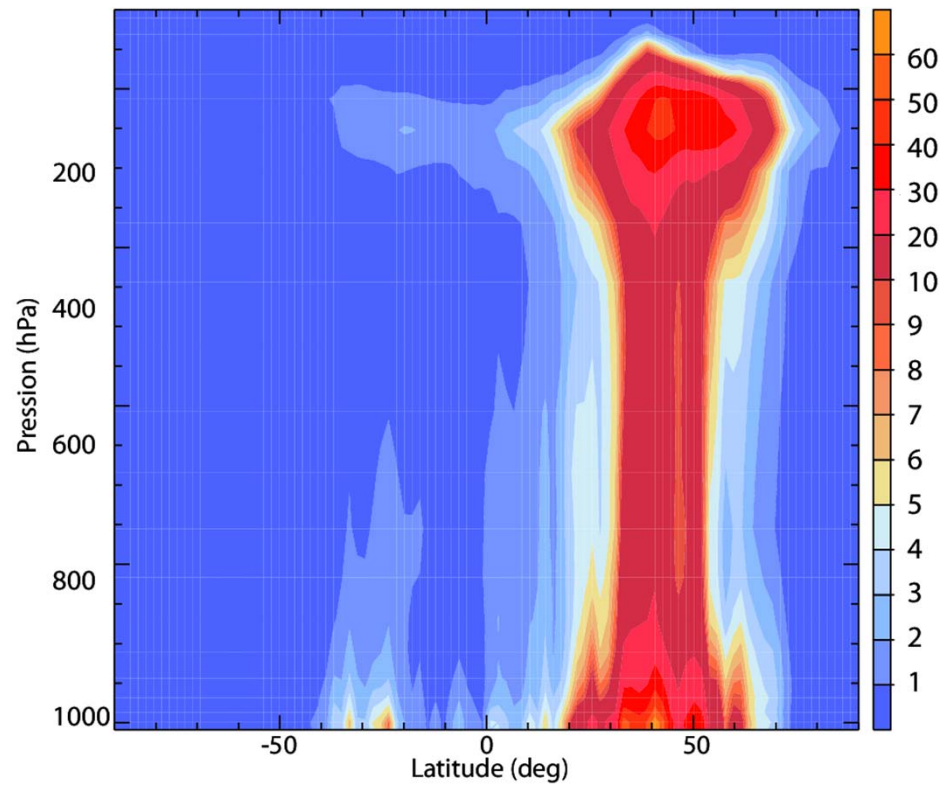
Distribution des flashes d'éclair détectés par les instruments LIS et OTD en janvier et juillet.

The contribution of NO_x sources to NO_x levels in the troposphere (%)

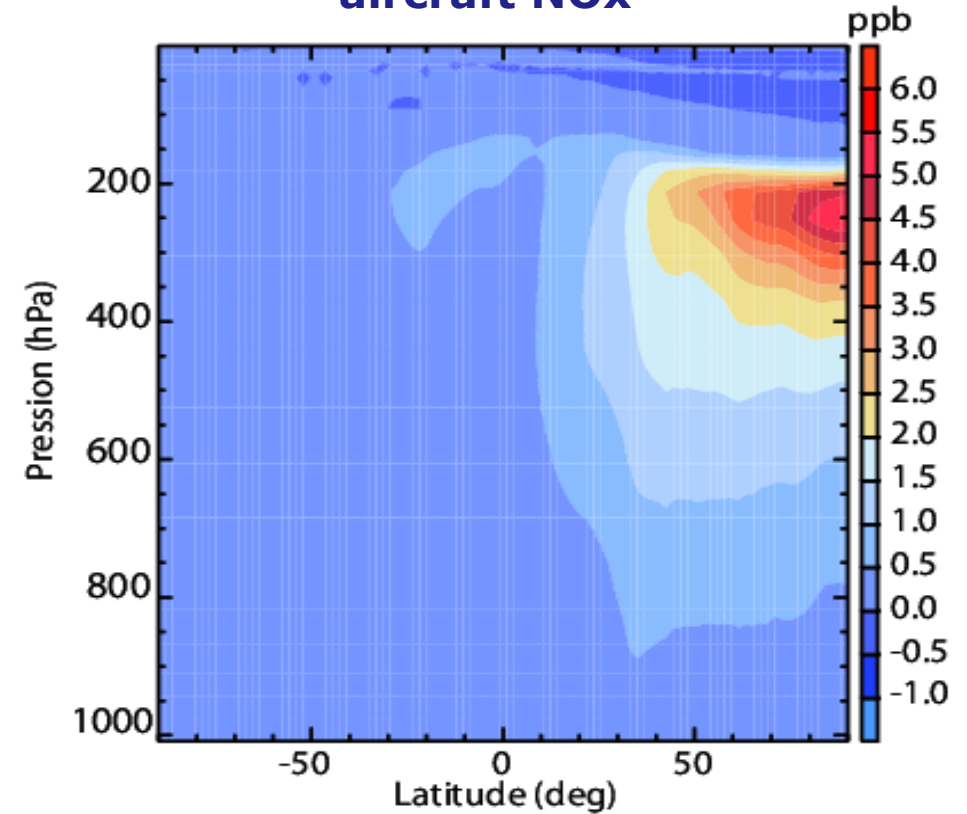


Nitrogen oxide emissions from the aircraft fleet

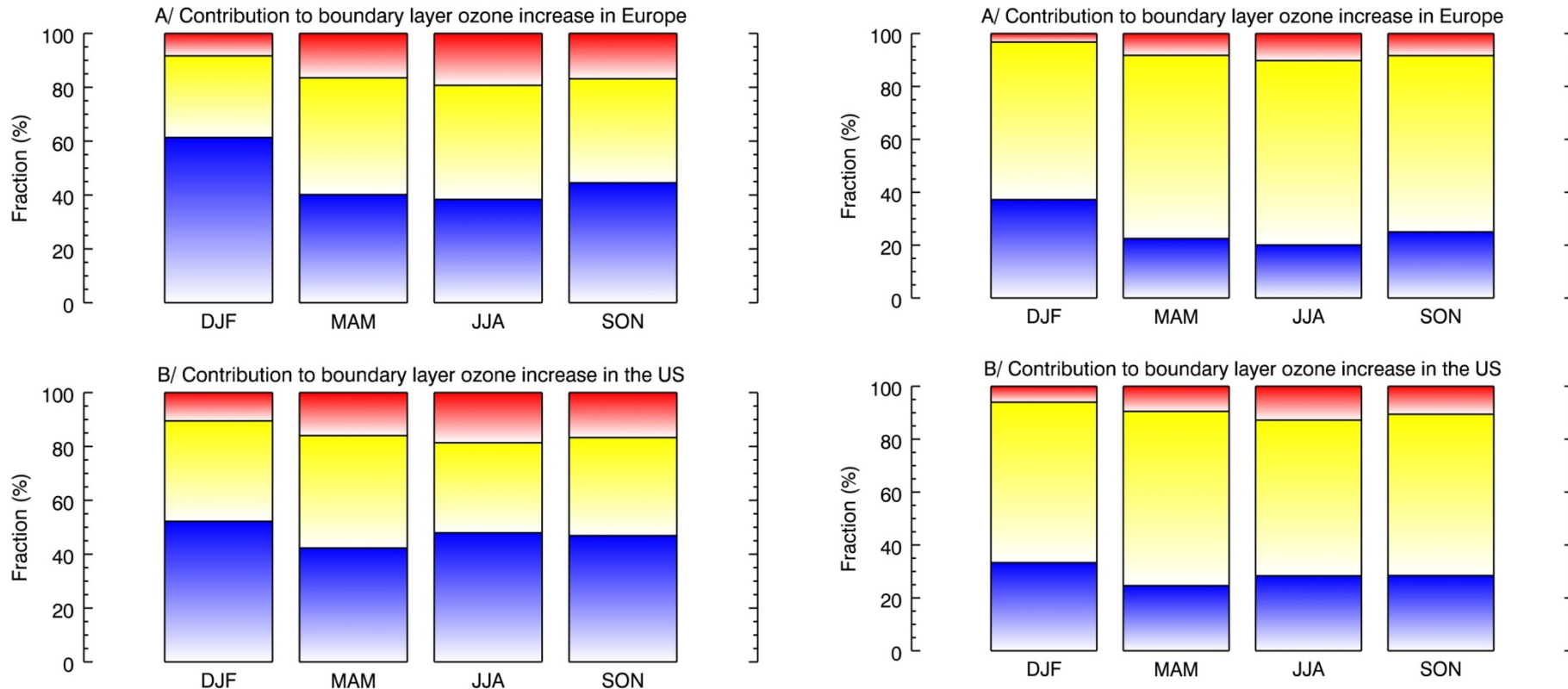
Fuel emissions from aircraft



Ozone perturbation from aircraft NO_x



Boundary layer ozone pollution from aircraft and shipping emissions

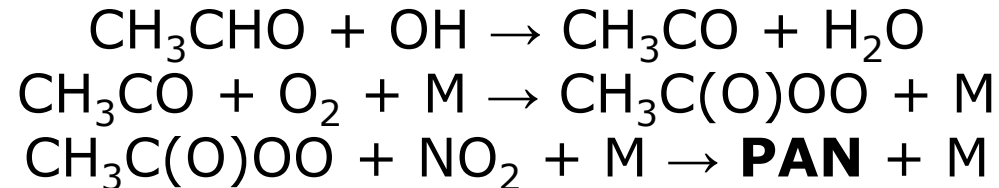


Relative contribution (%) of aircraft (blue), shipping (yellow), and road (red) emissions to boundary layer ozone increase due to transport in Europe and in the United States in 2050 under business as usual **scenario A1B (left)** and the mitigation scenario **B1 ACARE (right)**. The ozone change is integrated from the ground level to the pressure of 910 hPa (lowest three model levels).

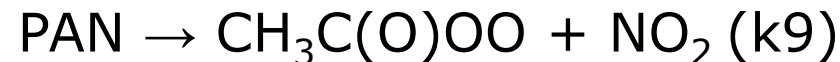
Hauglustaine and Koffi (2012)

Transport of NO_x to remote places

Nitrogen oxides have a short lifetime in the atmosphere (about a day or less at the surface) and cannot be transported over long distances. However, they can form reservoir species with longer lifetimes which can act as a source of NO_x in remote regions.

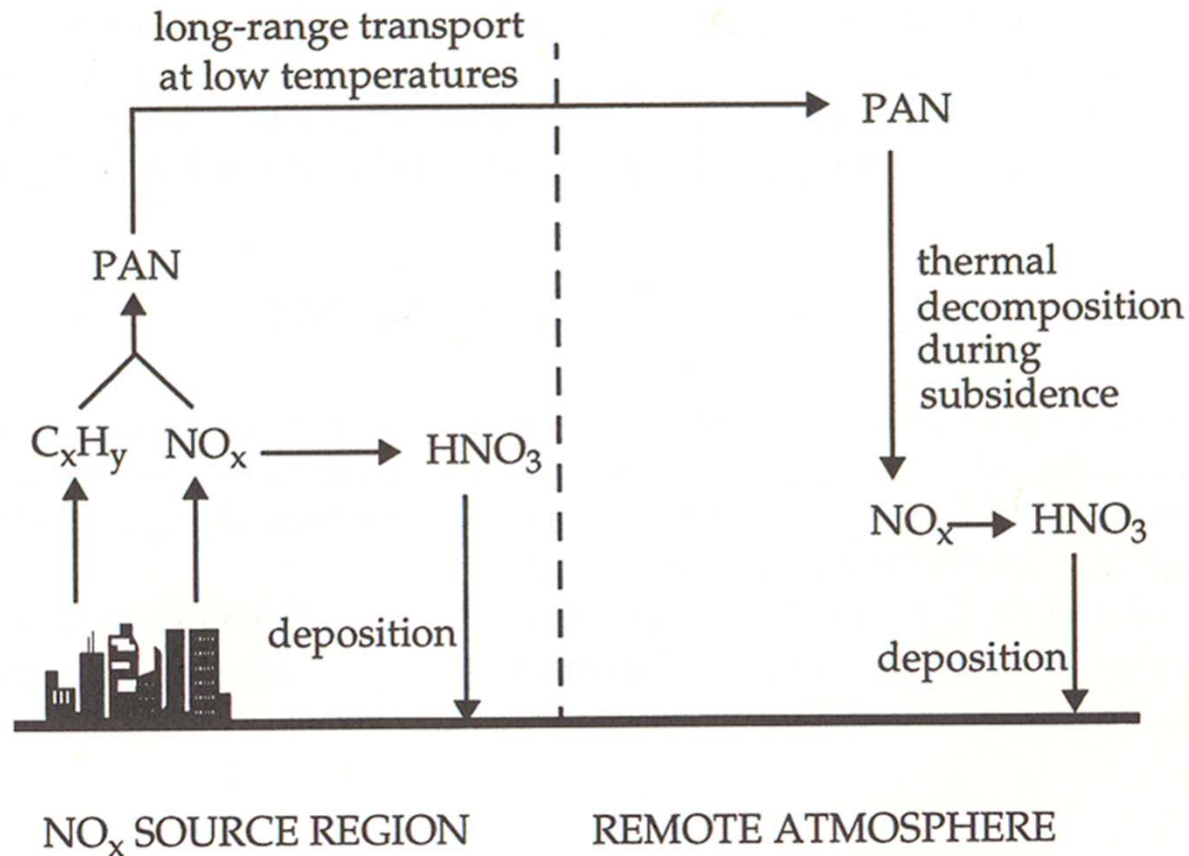


PAN : Peroxy Acetyl Nitrate



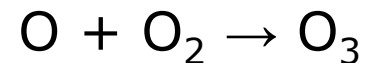
$$\begin{aligned} k_9 &= 3.6 \cdot 10^{-4} \text{ s}^{-1} \text{ à } 25^\circ\text{C} \quad (T=30 \text{ min}) \\ k_9 &= 1.2 \cdot 10^{-8} \text{ s}^{-1} \text{ à } -30^\circ\text{C} \quad (T=\text{several days}) \end{aligned}$$

Transport of NO_x to remote places



Schematic representation of the role of PAN as a source of NO_x to remote regions.

Equilibre photostationnaire O_3 -NO- NO_2 ($T \approx 1\text{min}$)

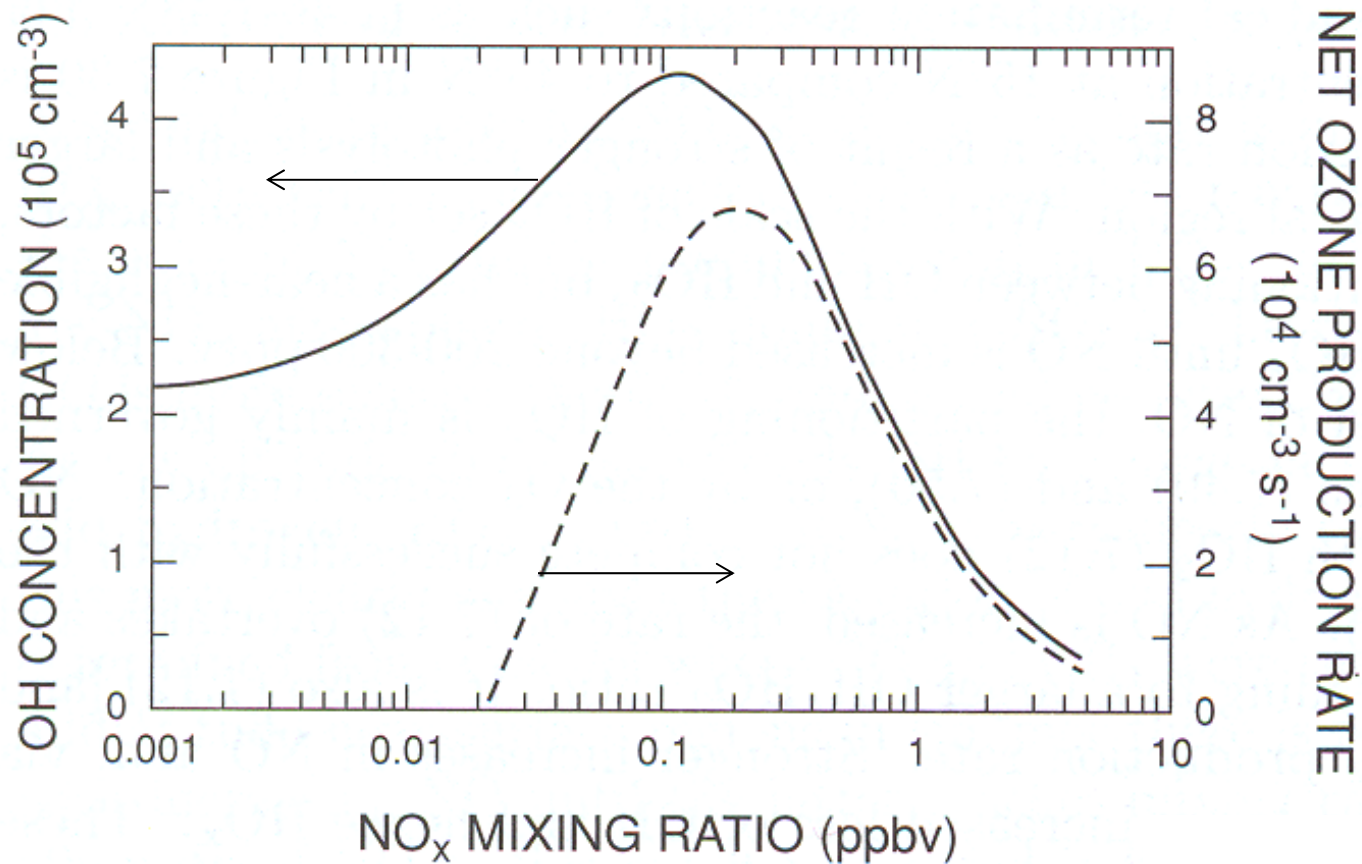


$$NO_2/NO = k_1 O_3 / j_{NO_2}$$

Production de l'ozone

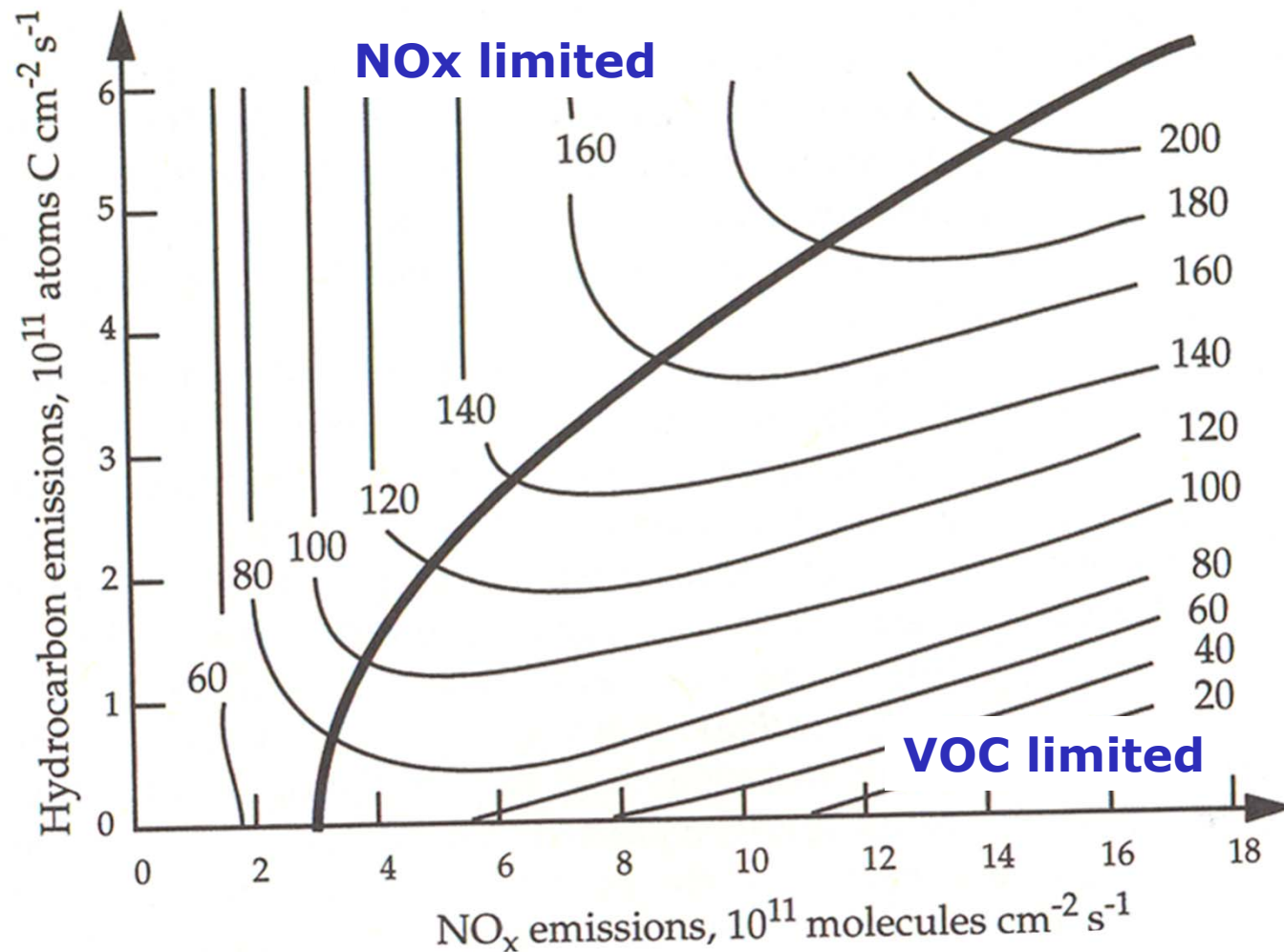


Photochemical regimes



OH concentration and ozone net photochemical production as a function of NO_x concentration.

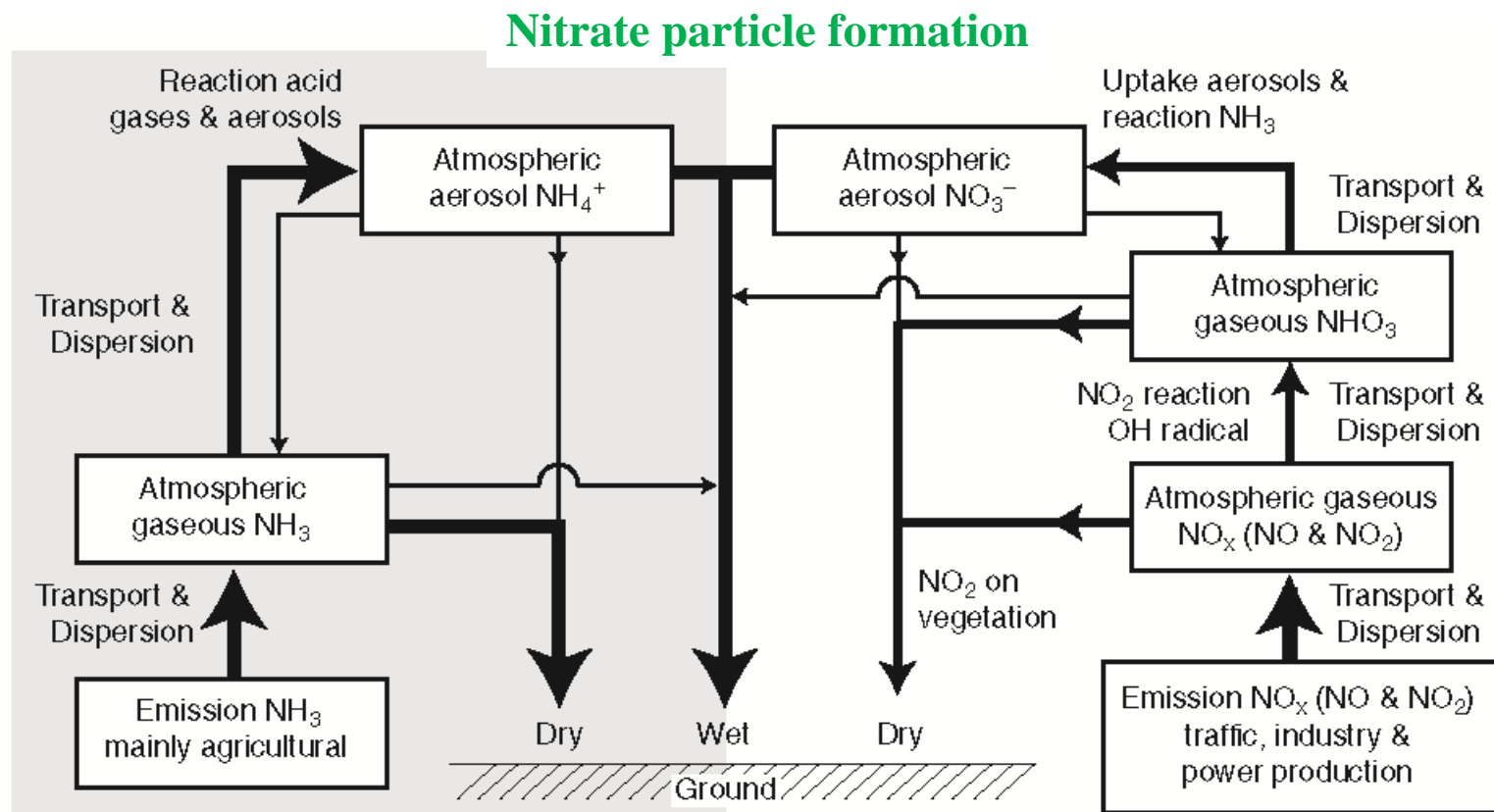
Photochemical regimes



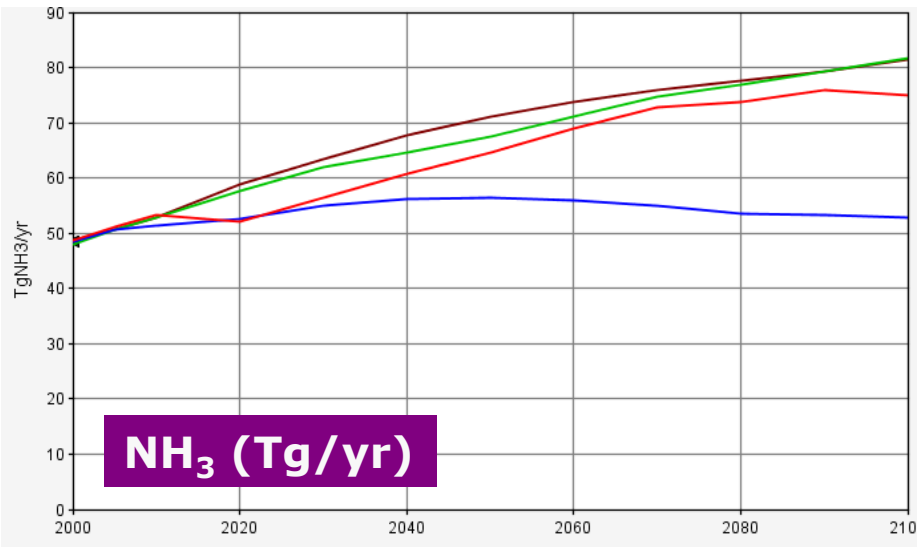
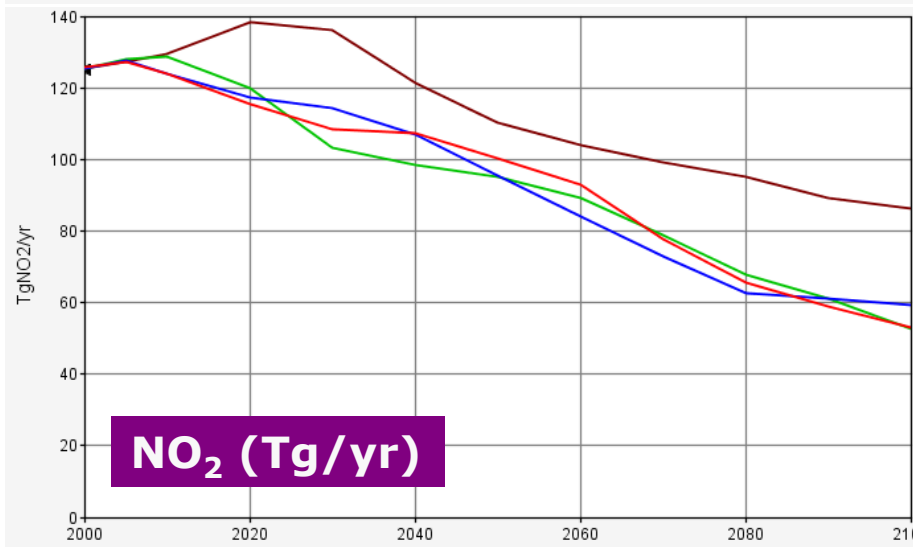
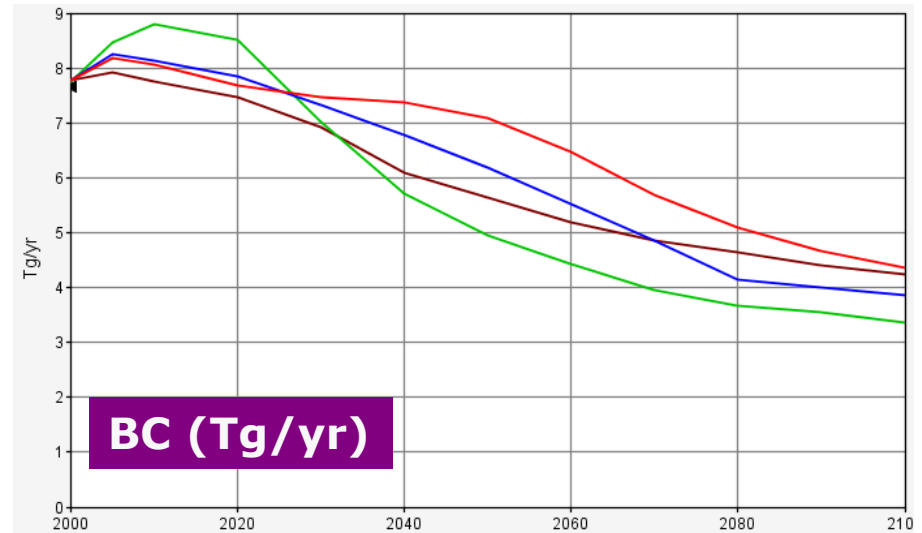
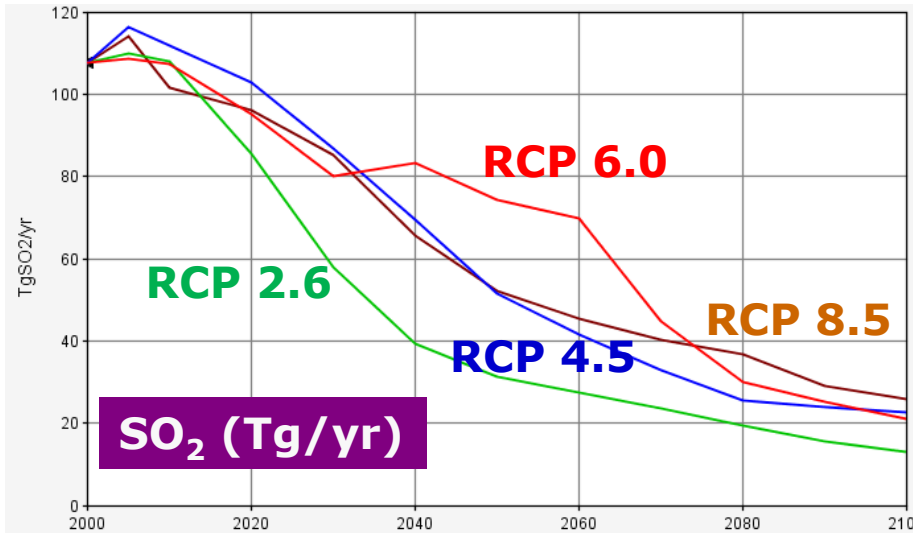
Ozone concentration ($\mu g/m^3$) as a function of NO_x and hydrocarbon emissions.

Ammonia and nitrates in the atmosphere

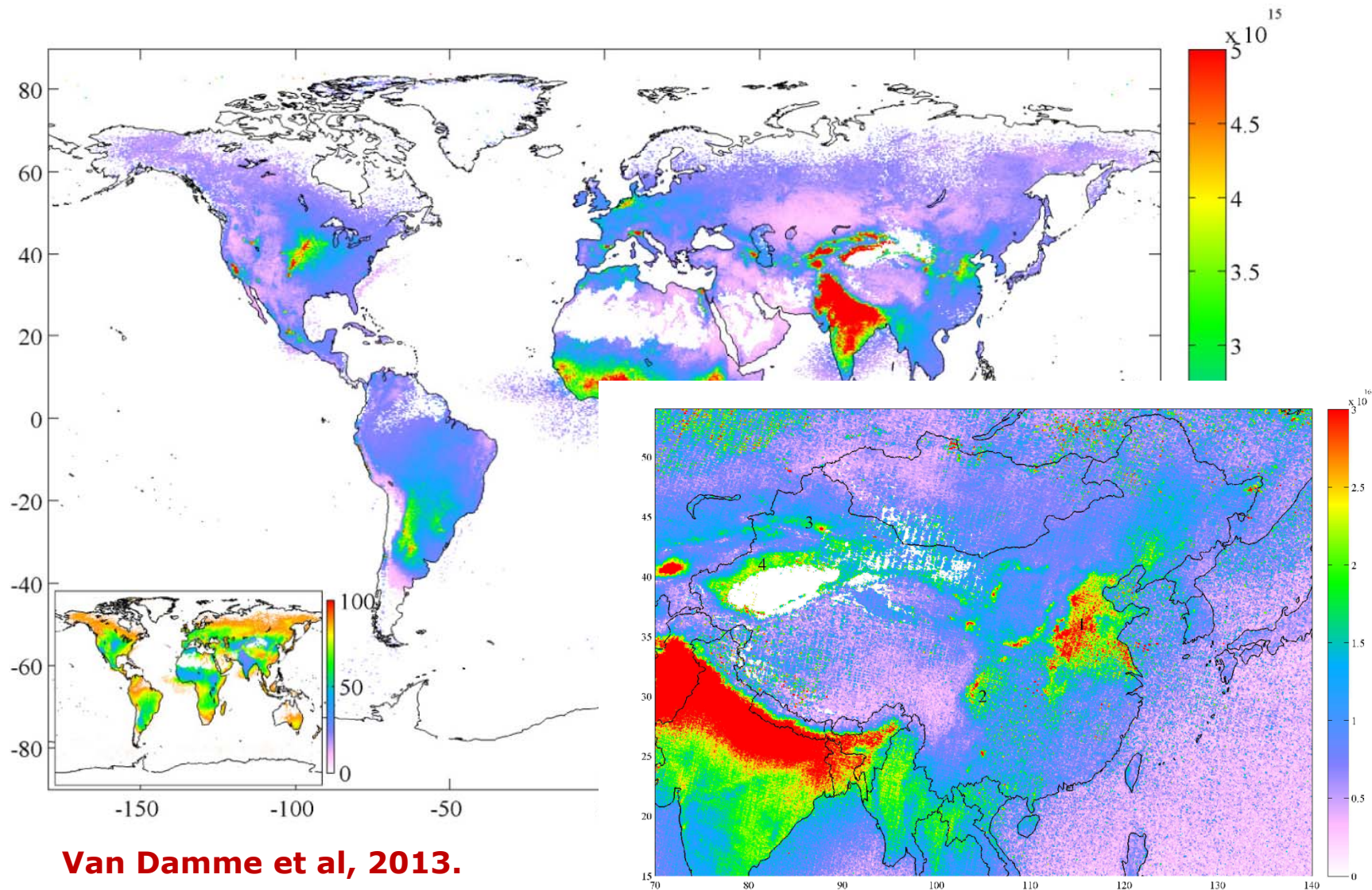
The formation of nitrate particles in the atmosphere arises from the reaction of reduced (left) and oxidized (right) nitrogen compounds involving both agricultural (NH_3) and fossil fuel burning (NO_x) emissions.



Representative Concentration Pathways (RCPs)



NH₃ column from space : IASI/METOP instrument



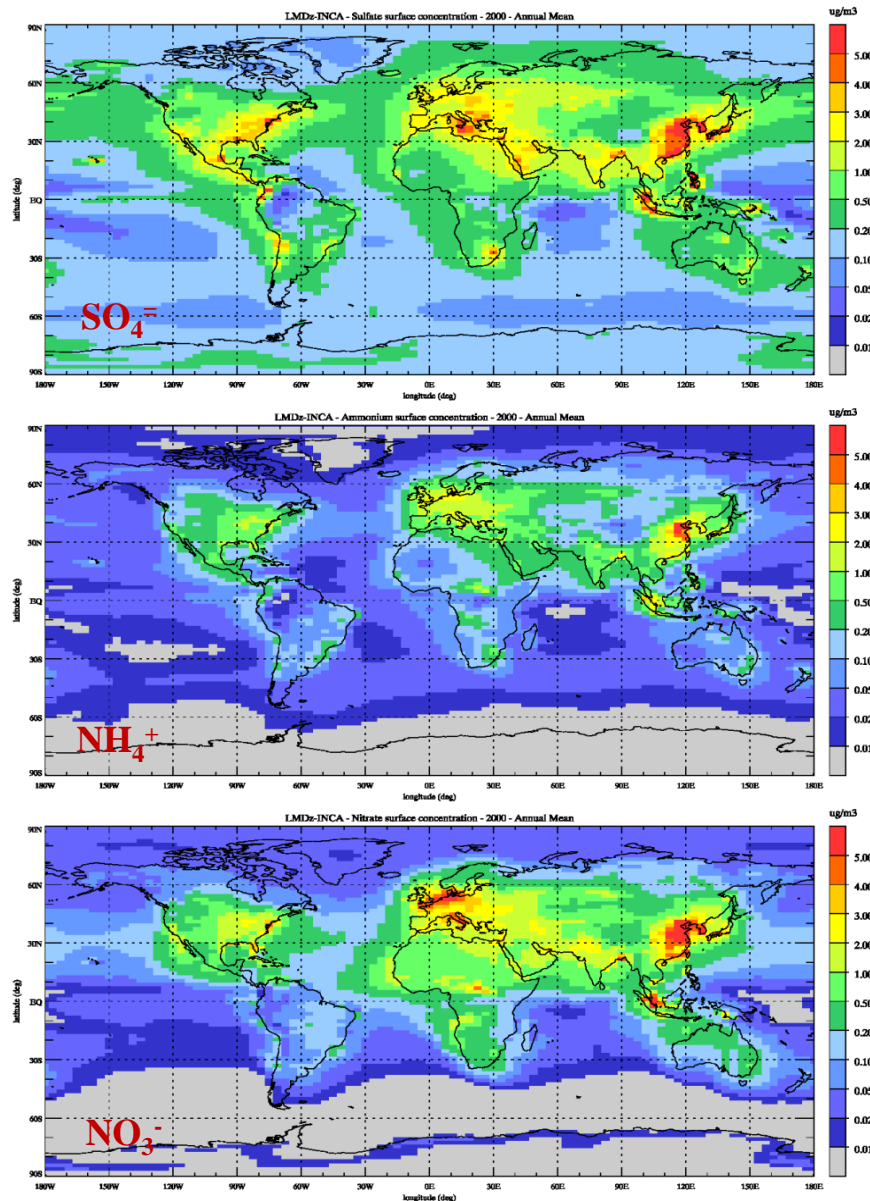
Van Damme et al, 2013.

Fig. 13. NH₃ distribution over eastern Asia (molec cm⁻²), following a gridding method explicitly accounting for the IASI footprint on each individual measurement. The distribution is a five-year error-weighted average of the IASI daytime total columns in the region (a post-filtering excluding cells with less than 10 observations has been carried out over land).

Nitrate particles and their impact on climate

- A series of modeling studies identified nitrate and ammonium particles as significant anthropogenic sources of aerosol load and estimated their direct radiative effect (e.g., Adams et al., 2001; Liao et al., 2003; Myhre et al., 2006; Feng and Penner, 2007). The radiative forcing associated with nitrates differs greatly among these earlier studies due for instance to the inclusion or not of coarse nitrate particles. The present-day forcing ranges in these earlier studies from -0.02 W/m^2 to -0.22 W/m^2 .
- Bauer et al. (2007) investigated the 2030 nitrate forcing based on the SRES A1B emission scenario. Coarse nitrate formation was not included. Present-day direct forcing of -0.11 W/m^2 increases to -0.14 W/m^2 in 2030.
- Bellouin et al. (2011) calculated the direct and first indirect nitrate forcings for the present (-0.17 W/m^2) and for the RCP scenarios and found that nitrates increase the total aerosol forcing by a factor of 2-4 in 2100. No coarse nitrates.
- Xu and Penner (2012) calculated recently the direct and first indirect forcings of nitrates for the present-day of respectively -0.12 W/m^2 and -0.09 W/m^2 (-0.21 W/m^2).
- Recently, Myhre et al. (2013) reported, based on AEROCOM, a direct present-day nitrate forcing of $-0.10 \pm 0.04 \text{ W/m}^2$ with a range among the models : -0.03 W/m^2 to -0.17 W/m^2 .

NH₃ cycle and nitrate formation in LMDz-INCA



NH₃ emissions based on ACCMIP and RCP scenarios (Lamarque et al., 2010, 2011). Natural emissions from GEIA. Gas phase chemistry of NH₃ and deposition processes.

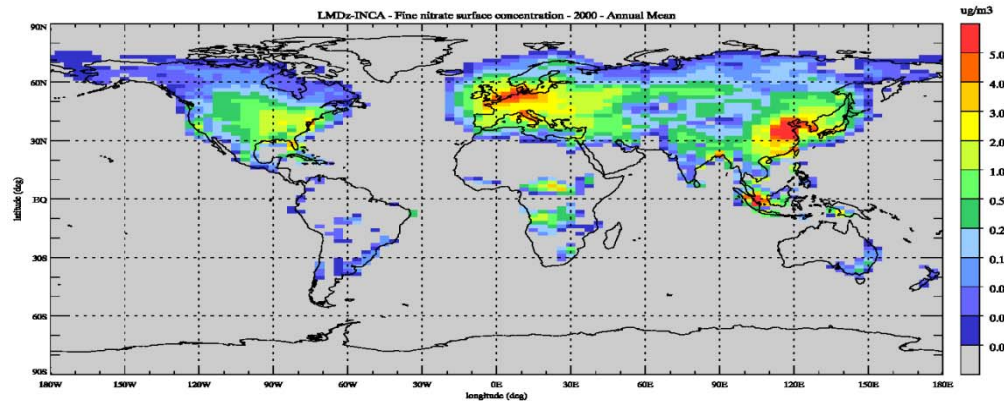
In the atmosphere NH₃ condenses on preexisting sulfate particles to form ammonium sulfate (NH₄)₂SO₄ or (NH₄)₃H(SO₄)₂ or NH₄HSO₄.

It can also react in the gas phase with HNO₃ to form new particles of NH₄NO₃. Equilibrium concentration calculated based on Seinfeld and Pandis (1998).

First order heterogeneous reactive uptake of HNO₃ to form coarse nitrates particles on preexisting dust and sea-salt particles.

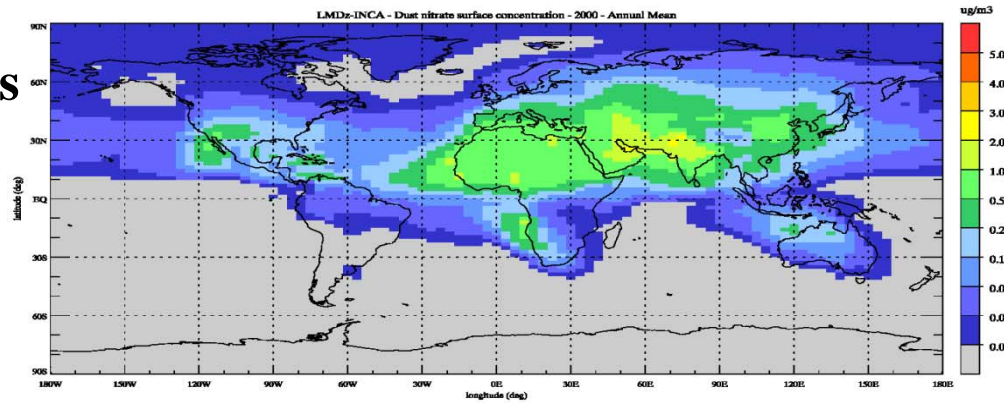
Fine and coarse nitrate surface concentrations ($\mu\text{g}/\text{m}^3$)

Fine mode nitrates



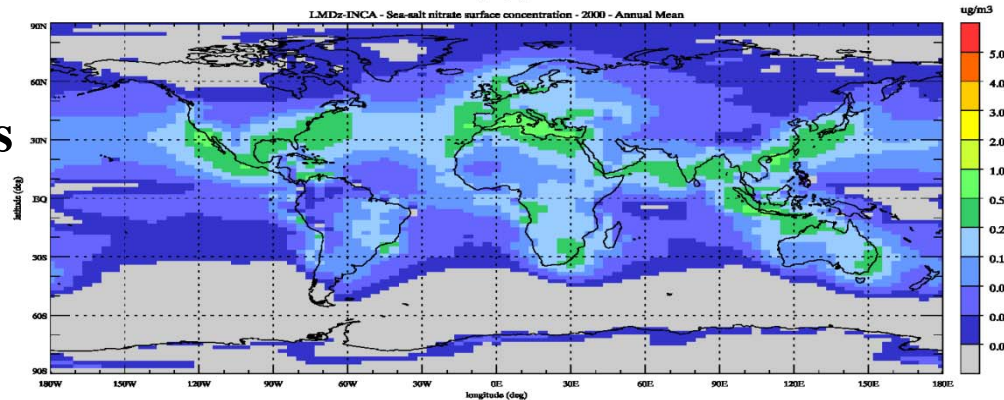
Burden:
0.05 TgN

Coarse mode nitrates
on dust particles



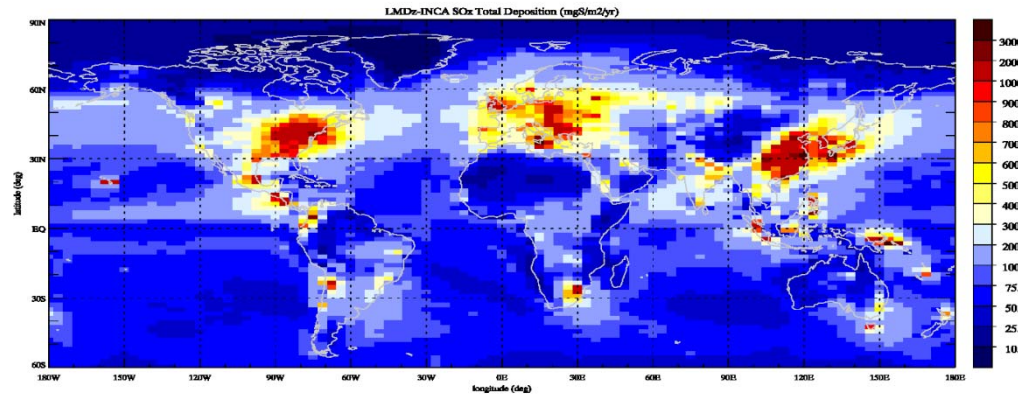
Burden:
0.07 TgN

Coarse mode nitrates
on sea-salt particles

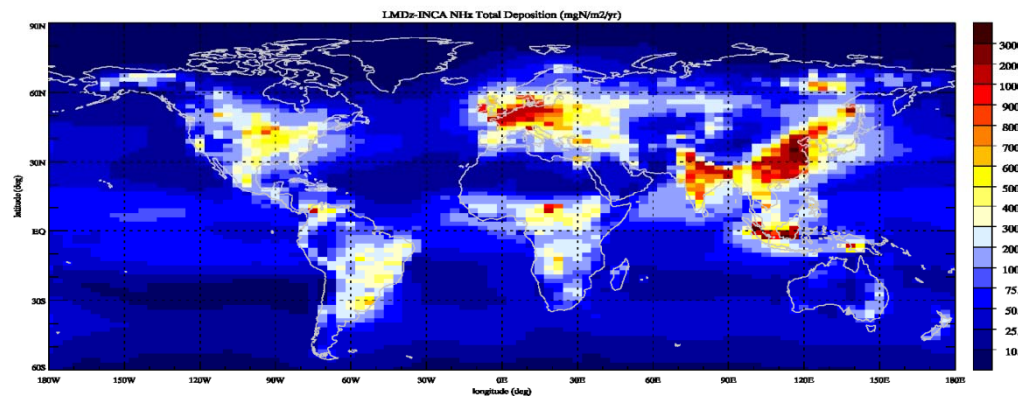


Burden:
0.06 TgN

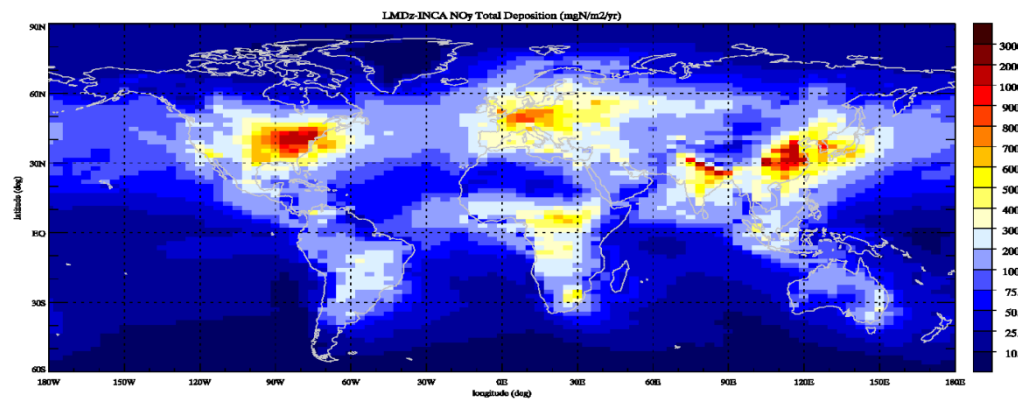
Nitrogen and sulfur total and annual surface deposition



SO₂ + SO₄⁻ deposition
107 TgS/yr

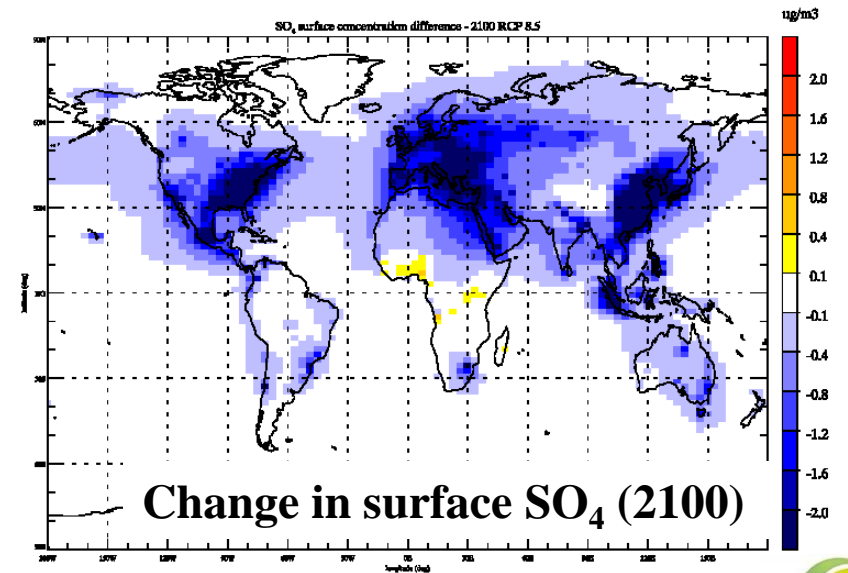
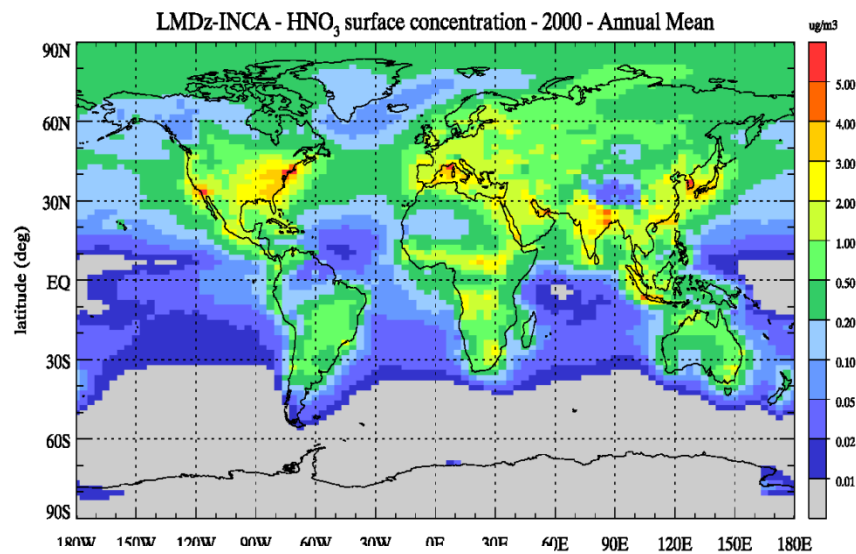
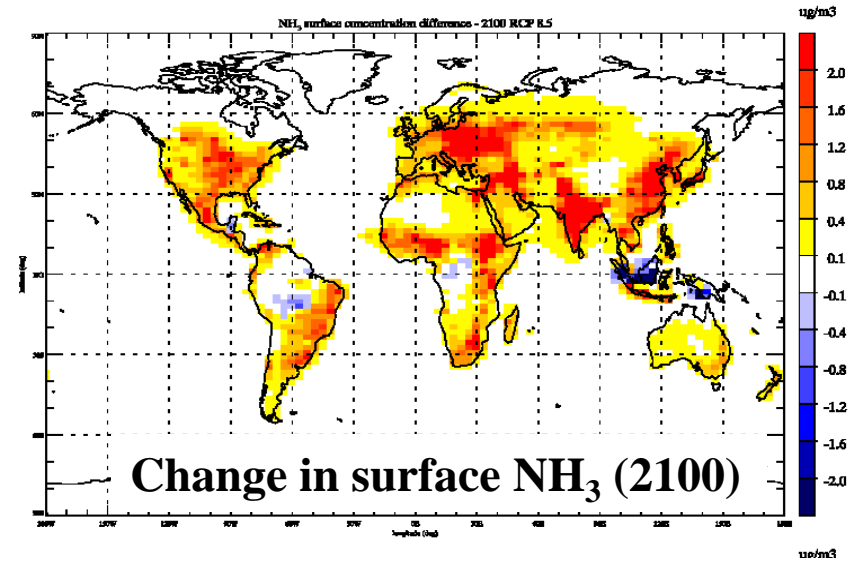
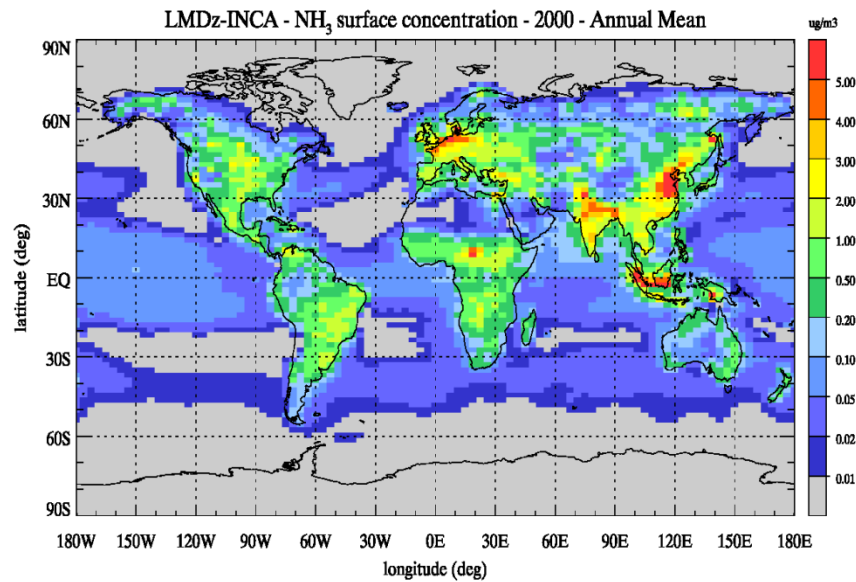


NH₃ + NH₄⁺ deposition
50 TgN/yr



NO_y + NO₃⁻ deposition
50 Tg N/yr

Future change in NO₃ precursor surface concentrations (μg/m³) – RCP8.5



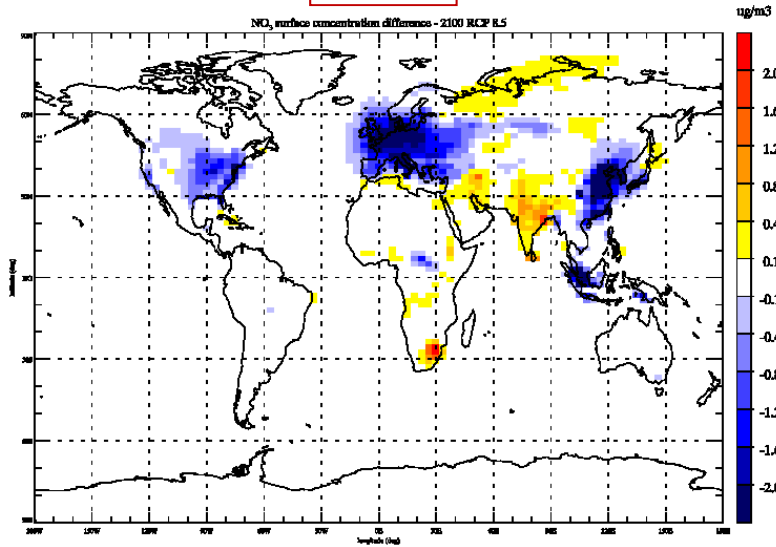
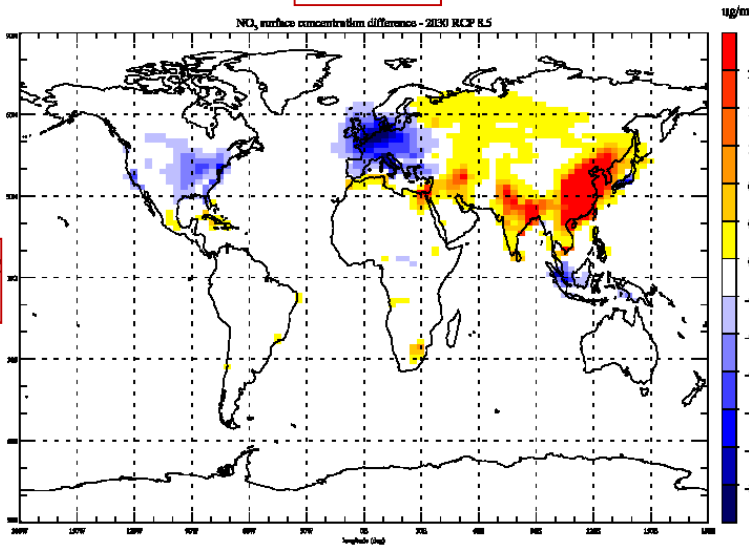
Hauglustaine et al., ACPD, 2014.

Evolution of nitrate surface concentration ($\mu\text{g}/\text{m}^3$)

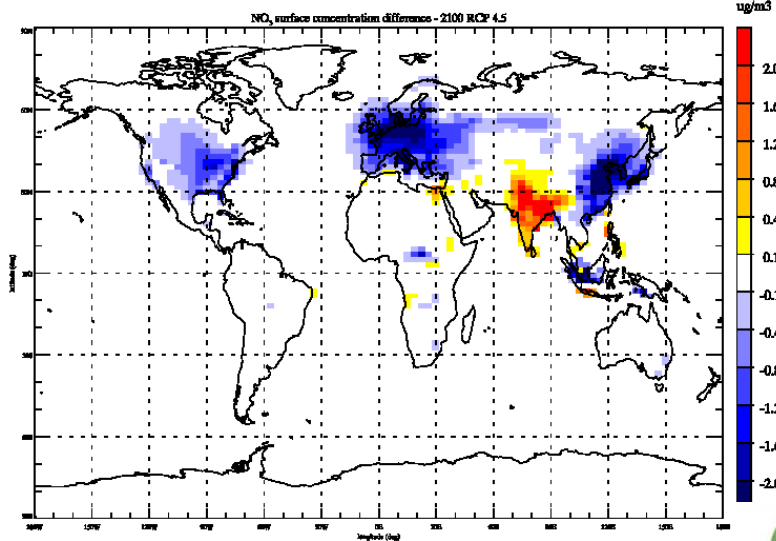
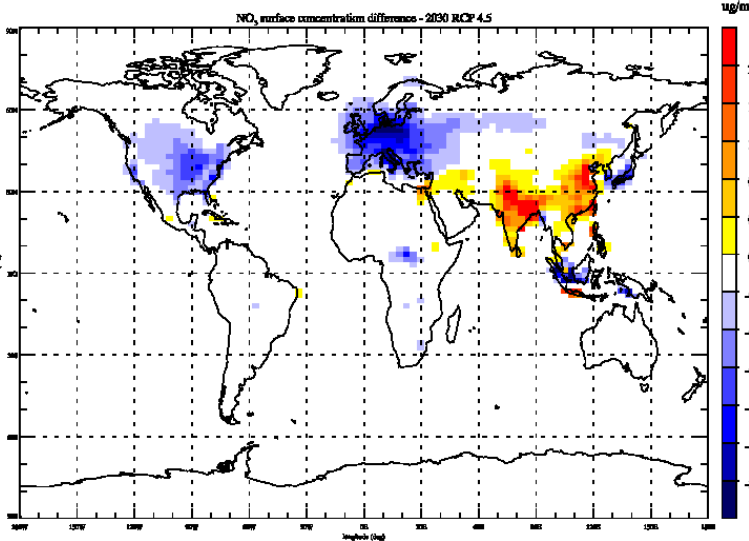
2030

2100

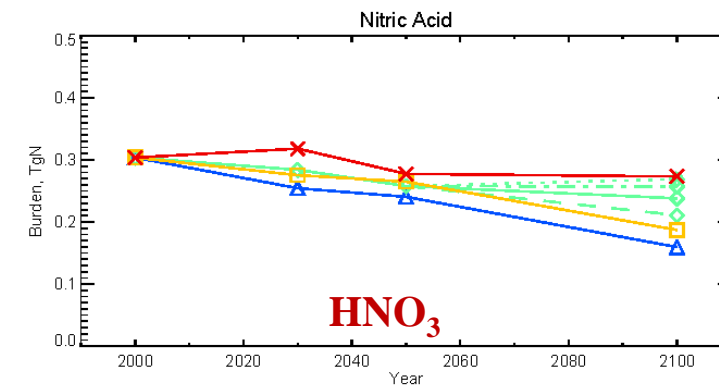
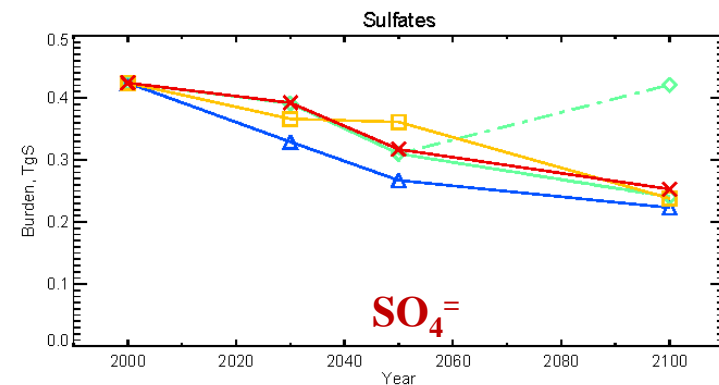
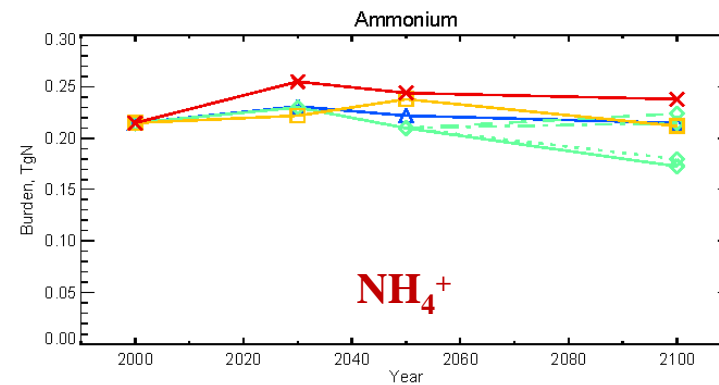
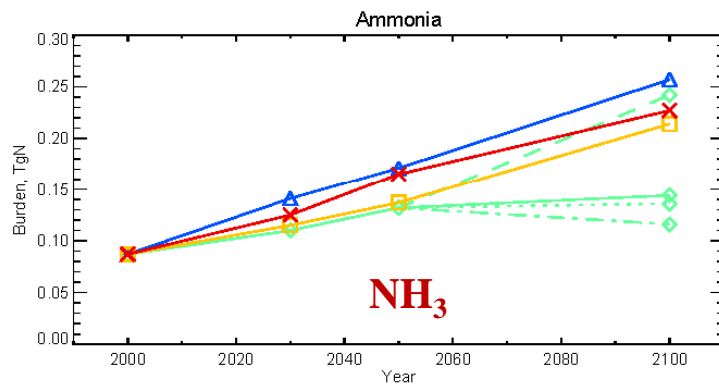
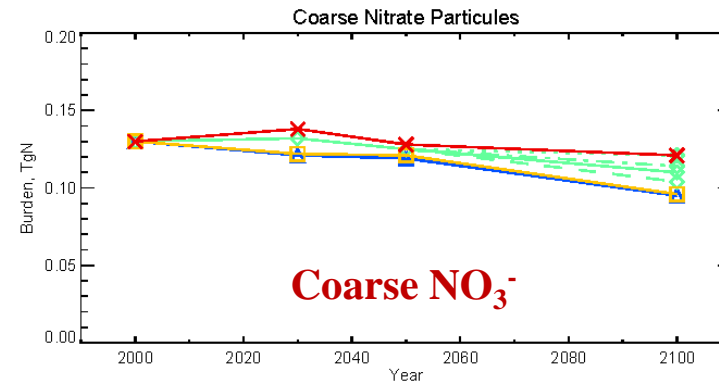
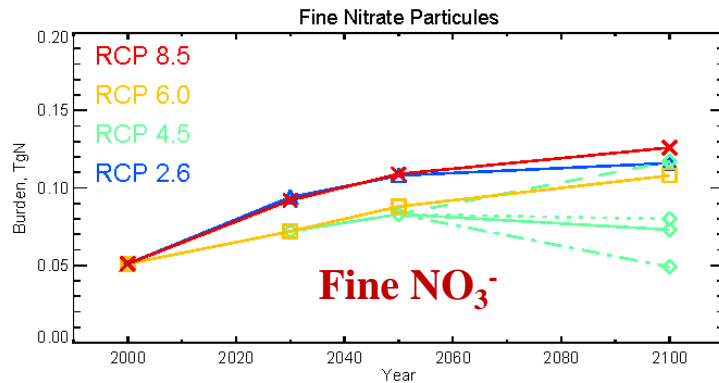
RCP8.5



RCP4.5



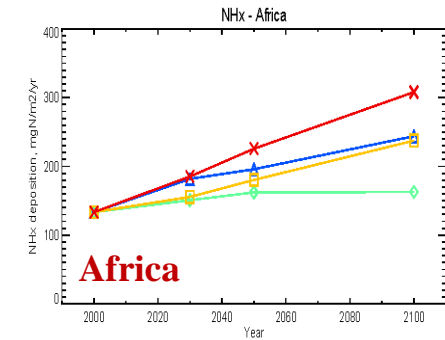
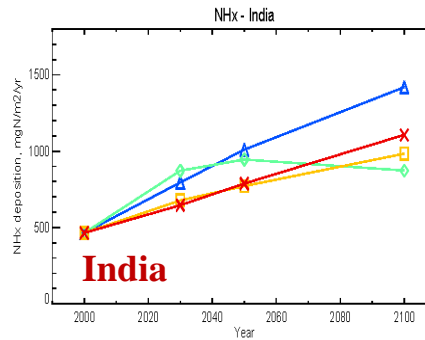
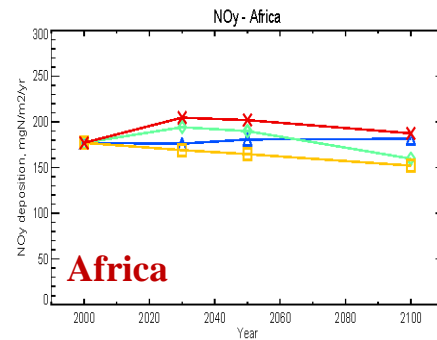
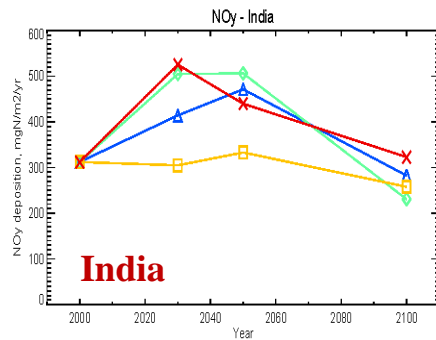
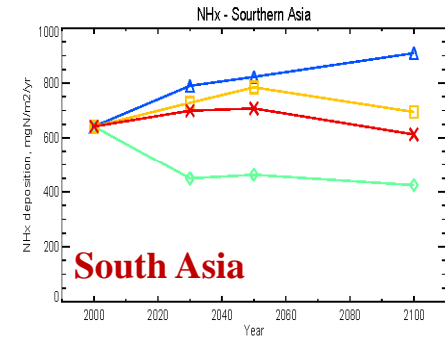
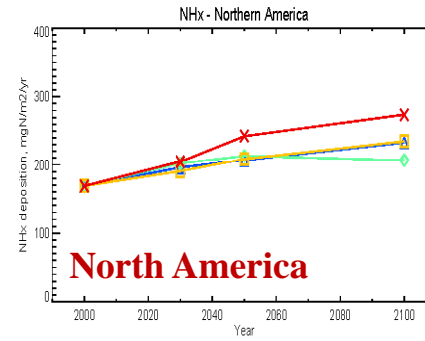
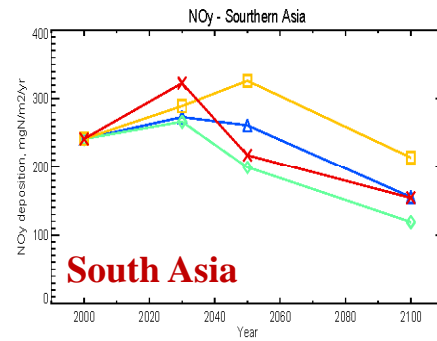
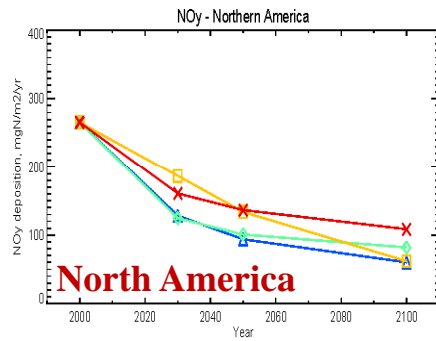
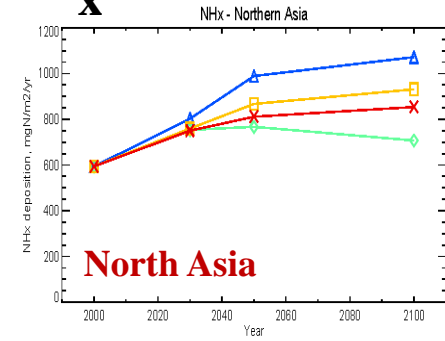
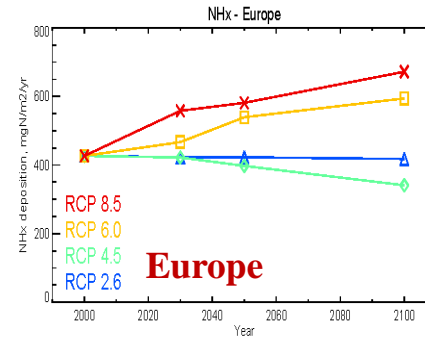
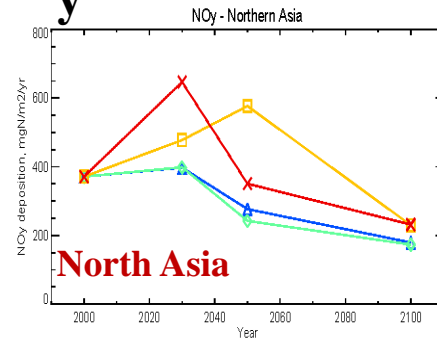
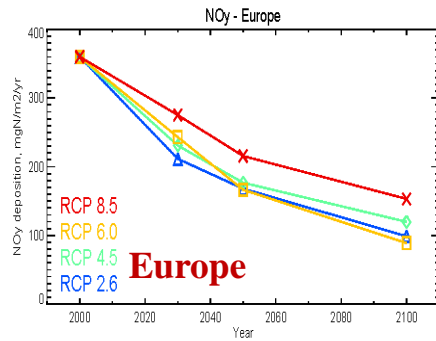
Evolution of nitrate and its precursors (burden, TgN)



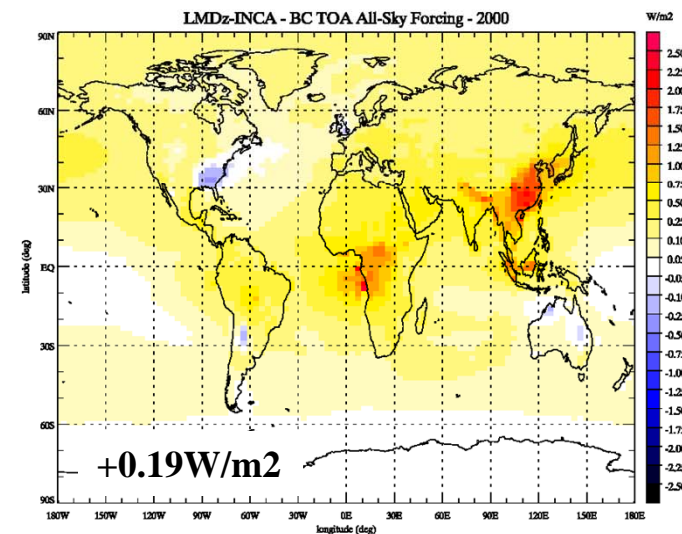
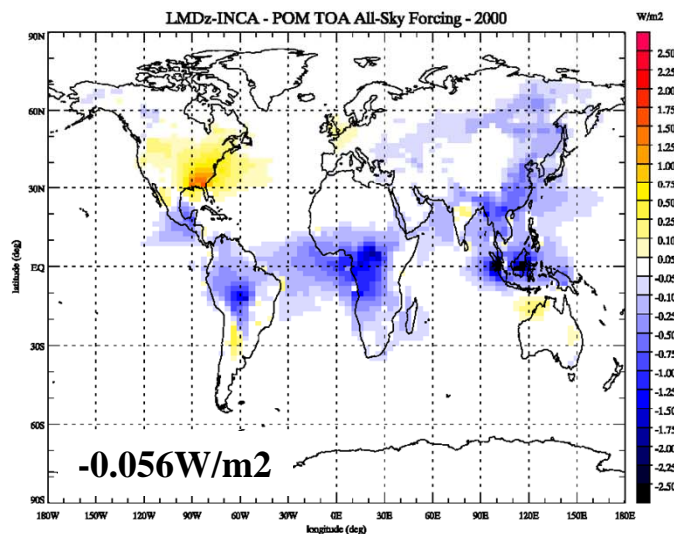
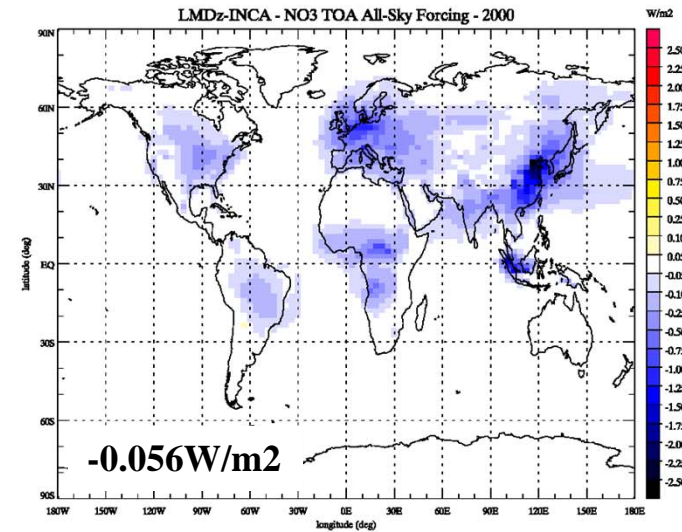
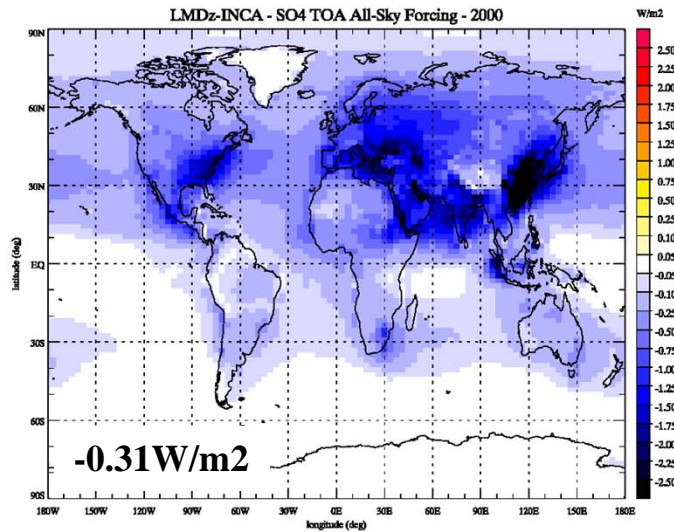
Evolution of NO_y and NH_x surface deposition (TgN)

NO_y

NH_x



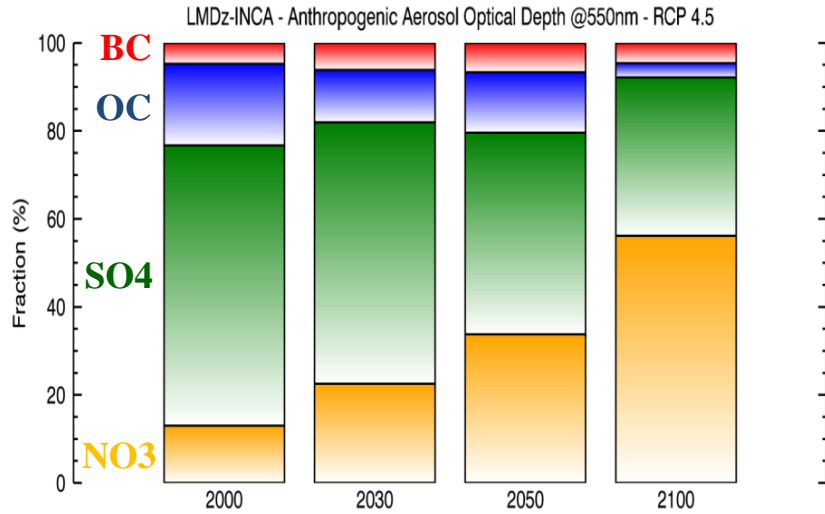
Aerosol direct radiative forcings (W/m^2) – 1850-2000



Hauglustaine et al., ACPD, 2014.

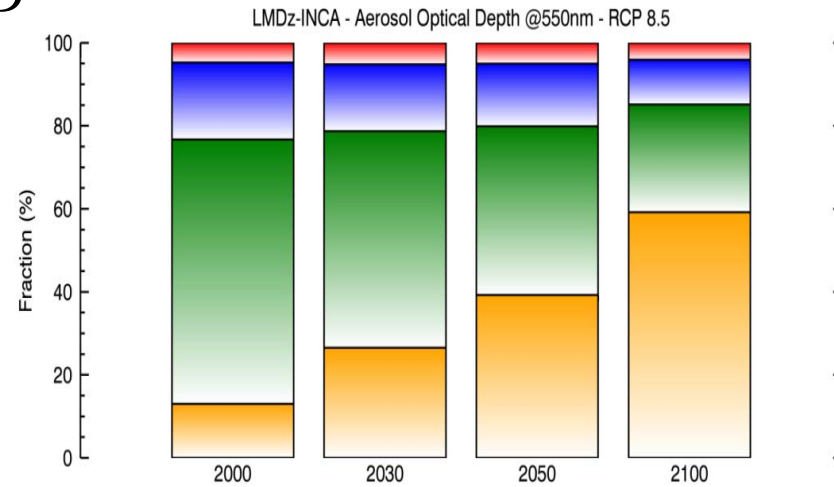
Evolution of aerosol direct radiative forcings (W/m^2)

Scénario RCP 4.5



AOD

Scénario RCP 8.5



Nitrogen emissions and their impact on European radiative forcings

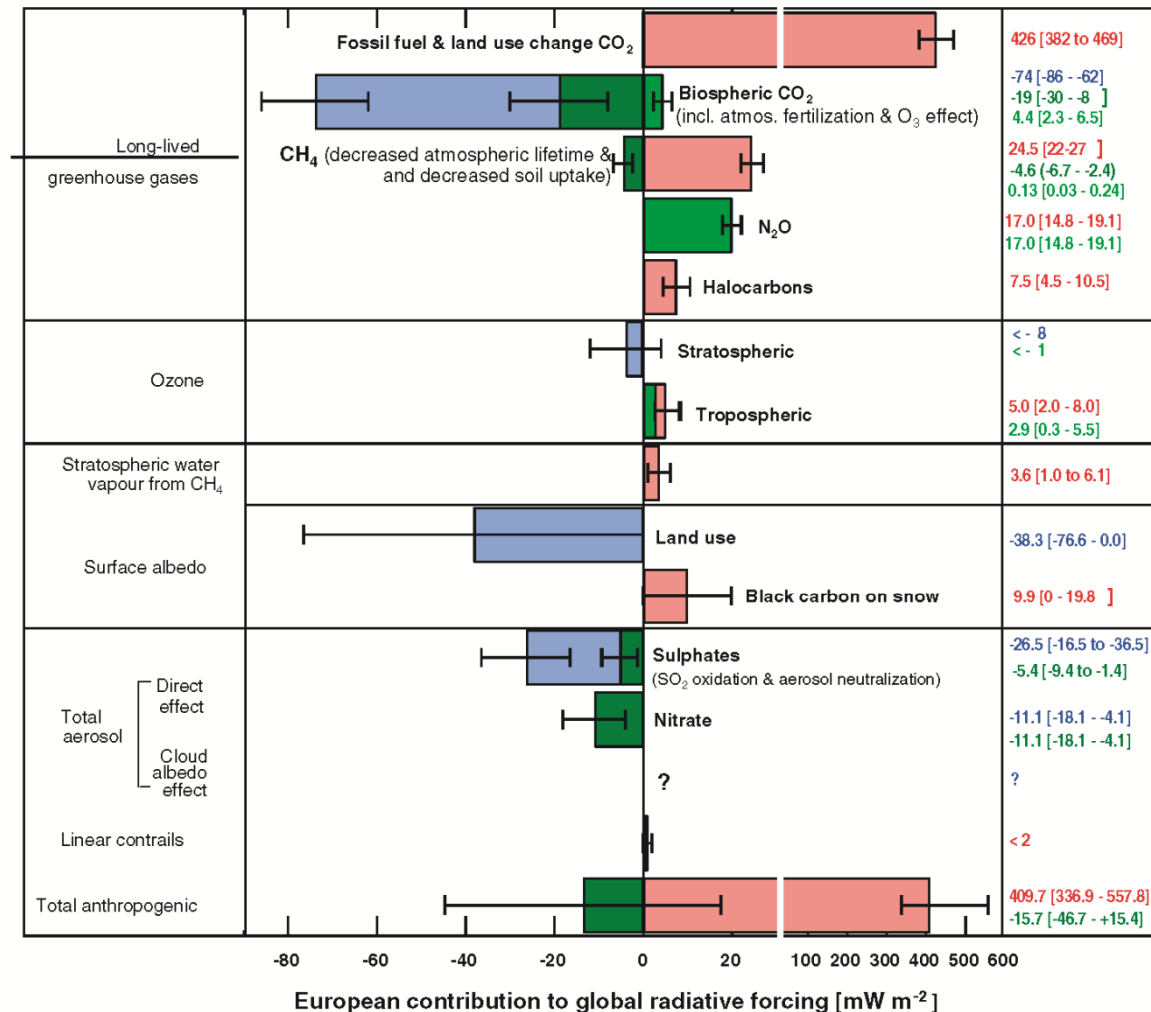


Figure 19.5 A first estimate of the change in global radiative forcing (RF) due to European emissions and the effect on European anthropogenic N_x emissions to the atmosphere. The RF components due to European anthropogenic activity have been derived as described in the text. The N_x effect is taken from Table 19.8. Red bars: positive radiative forcing; light green bars: positive radiative forcing due to direct/indirect effects of N_x; blue bars: negative radiative forcing; dark green bars: negative radiative forcing due to direct / indirect effects of N_x. For biospheric CO₂, the dark green bar represents the additional CO₂ sequestered by forests and grasslands due to N_x deposition, while the light green bar represents the decrease in productivity due to effects of enhanced O₃ caused by NO_x emissions. For CH₄ the positive (not visible) and negative contributions represent the effects of N_x in reducing CH₄ uptakes by soil and the decreased atmospheric lifetime, respectively.

Nitrogen emissions and their environmental impact

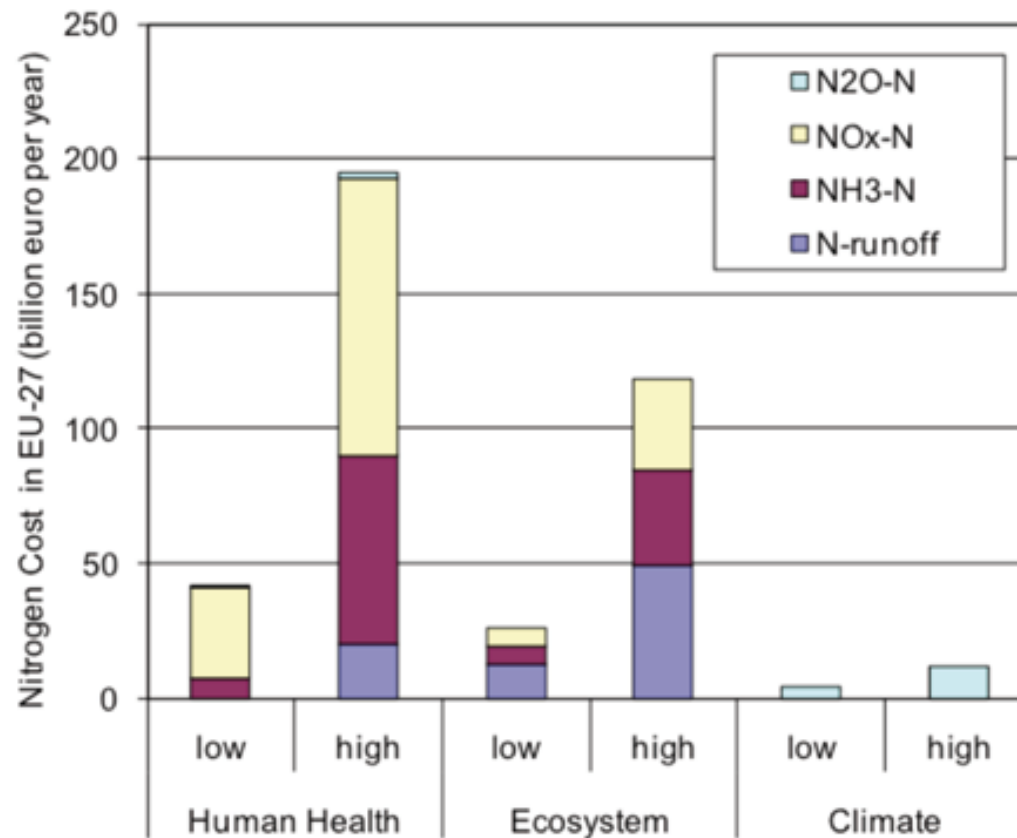


Figure 4.3 Estimated environmental costs due to reactive nitrogen emissions to air and to water in the EU-27 (Brink et al. 2011; Sutton et al. 2011c)